

Spatial Precoder Design for Space-Time Coded MIMO Systems: Based on Fixed Parameters of MIMO Channels

Tharaka A. Lamahewa, Rodney A. Kennedy, Thushara D. Abhayapala, Van K. Nguyen

Abstract—In this paper, we introduce the novel use of linear spatial precoding based on fixed and known parameters of multiple-input multiple-output (MIMO) channels to improve the performance of space-time coded MIMO systems. We derive linear spatial precoding schemes for both coherent (channel is known at the receiver) and non-coherent (channel is unknown at the receiver) space-time coded MIMO systems. Antenna spacing and antenna placement (geometry) are considered as fixed parameters of MIMO channels, which are readily known at the transmitter. These precoding schemes exploit the antenna placement information at both ends of the MIMO channel to ameliorate the effect of non-ideal antenna placement on the performance of space-time coded systems. In these schemes, the precoder is fixed for given transmit and receive antenna configurations and transmitter does not require any feedback of channel state information (partial or full) from the receiver. Closed form solutions for both precoding schemes are presented for systems with up to three receiver antennas. A generalized method is proposed for more than three receiver antennas. We use the coherent space-time block codes (STBC) and differential space-time block codes to analyze the performance of proposed precoding schemes. Simulation results show that at low SNRs, both precoders give significant performance improvement over a non-precoded system for small antenna aperture sizes.

Index Terms—Space-time coding, channel modelling, linear precoder design, MIMO systems, non-isotropic scattering, spatial correlation.

I. INTRODUCTION

MIMO communication systems that use multi-antenna arrays simultaneously during transmission and reception have generated significant interest in recent years. Under the assumption of fading channel coefficients between different antenna elements are statistically independent and fully known at the receiver (coherent detection), theoretical work of [1] and [2] revealed that the channel capacity of multiple-antenna array communication systems scales linearly with the smaller of the number of transmit and receive antennas. Motivated

This work was supported by the Australian Research Council Discovery Grant DP0343804.

T. A. Lamahewa, R. A. Kennedy and T. D. Abhayapala are with the Department of Information Engineering, Research School of Information Sciences and Engineering, The Australian National University, Canberra ACT 0200, Australia. email: {tharaka.lamahewa, rodney.kennedy, thushara.abhayapala}@anu.edu.au. R. A. Kennedy and T. D. Abhayapala are also with National ICT Australia, Locked Bag 8001, Canberra, ACT 2601, Australia. National ICT Australia is funded through the Australian Government's *Backing Australia's Ability* initiative, in part through the Australian Research Council. V. K. Nguyen is with the School of Engineering and Technology, Deakin University, Geelong, VIC 3217, Australia. email: vknguyen@deakin.edu.au.

Part of this paper has been presented in APCC-2005, Perth, Australia.

by these works, [3–5] have proposed several modulation and coding schemes, namely space-time trellis codes and space-time block codes, to exploit the potential increase in capacity and diversity gains using multi antenna arrays with coherent detection.

The effectiveness of these coherent space-time coding schemes mainly relies on the accuracy of the channel estimation at the receiver. Therefore, differential space-time coding (DSTC) schemes proposed in [6–8] make an attractive alternative to combat inaccuracy of channel estimation in coherent space-time coding schemes. With DSTC schemes, channel state information is not required at either end of the channel. However, it is well known that DSTC schemes suffer a 3dB performance loss compared to space-time coding schemes with coherent detection at the receiver.

For both schemes, code structures are designed assuming that the channel gains between the transmitter and receiver antennas undergo uncorrelated independent flat fading. Such an assumption is valid only if the scattering environment is isotropic, i.e., scattering is uniformly distributed over the receiver and transmitter antenna arrays, and also only if the antennas in an array are well separated. Recent studies have shown that insufficient antenna spacing and non-isotropic scattering reduce the performance of space-time coded communication systems [9–11]. This has motivated the design of linear precoders for space-time coded multiple antenna systems by exploiting the statistical information of the MIMO channels [12–17]. In these schemes, the receiver either feeds back the full channel state information or the correlation coefficients of the channel (covariance feedback) to the transmitter via a low rate feedback channel. In order to be cost effective and optimal, these designs assumed that the channel remains stationary (channel statistics are invariant) for a large number of symbol periods and the transmitter is capable of acquiring robust channel state information. However, when the channel is non-stationary or it is stationary for a small number of symbol periods, the receiver will have to feedback the channel information to the transmitter frequently. As a result, the system becomes costly and the optimum precoder design, based on the previously possessed information, becomes outdated quickly. In some circumstances feeding back channel information is not possible. These facts have motivated us to design a precoding scheme based on fixed and known parameters of the underlying MIMO channel. Following list summarizes the original contributions of this paper.

- By exploiting the spatial dimension of a MIMO channel,

we design linear spatial precoding schemes to improve the performance of coherent and differential space-time block coded systems. These linear spatial precoders are designed based on previously unutilized fixed and known parameters of MIMO channels, the antenna spacing and antenna placement details. We use the spatial channel decomposition given in [18] to incorporate the antenna spacing and antenna placement details into the precoder design.

- Both precoders are fixed for fixed¹ antenna placement and the transmitter does not require any form of feedback of channel state information (partial or full) from the receiver.
- Since the designs are based on fixed parameters, these spatial precoders can be used in non-stationary channels as well as stationary channels.
- Upper bounds for pairwise error probability (PEP) of coherent space-time codes and differential space-time codes are derived for spatially correlated MIMO channels. To the authors knowledge, the PEP upper bound of differential space-time codes is a new bound. Utilizing the MIMO channel decomposition given in [18], antenna configuration details and scattering environment parameters (angular spreads and mean angle of arrival and departure) are incorporated in to these PEP upper bounds. Assuming an isotropic scattering environment surrounding the transmitter and receiver antenna arrays, we minimize the two PEP upper bounds to obtain the optimum precoders.
- We show that our spatial precoding schemes reduce the effect of non-ideal antenna placement, which is a major contributor to the spatial correlation, on the MIMO system performance. In these schemes, the precoder virtually arranges the antennas into an optimal configuration as such the spatial correlation between all antenna elements is reduced.
- The precoder design is based on the spatial channel model proposed in [18], but we show that the performance of both precoding schemes does not depend on the channel model that used to model the underlying MIMO channel. Therefore, our design and simulation results provide an independent confirmation of the validity and usefulness of the channel model proposed in [18].

An outline of the paper is as follows. Section II reviews the spatial channel model used in our design. In Section III, the precoded coherent STBC and differential STBC systems are described along with detection rules at the receiver. Sections IV and V present the optimization problem and the optimal precoder solution for coherent STBC and differential STBC, respectively. For both precoding schemes, we show that the optimum linear precoder for a multiple-input single-output (MISO) fading channel is essentially given by the classical “water-filling” strategy found in information theory [1]. For a MIMO channel, the linear precoder is determined by a novel generalized water-filling scheme. Closed form solutions for both precoding schemes are presented for systems with up

¹antennas are fixed relative to each other

to three receiver antennas. A generalized method is proposed for more than three receiver antennas. Sections VI and VII present results obtained with proposed precoding schemes for various spatial scenarios using the spatial channel model in [18] as the underlying MIMO channel. Section VII also presents results obtained with proposed precoding scheme for non-isotropic scattering environments (i.e., limited angular spreads at the transmitter and receiver antenna arrays). Section VIII gives the simulation results of our proposed precoding scheme applied on other statistical channel models found in the literature. Section IX present some concluding remarks and five appendices contain various proofs.

Notations: Throughout the paper, the following notations will be used: Bold lower (upper) letters denote vectors (matrices). $[\cdot]^T$, $[\cdot]^*$ and $[\cdot]^\dagger$ denote the transpose, complex conjugate and conjugate transpose operations, respectively. The symbols $\delta(\cdot)$ and \otimes denote the Dirac delta function and Matrix Kronecker product, respectively. The notation $E\{\cdot\}$ denotes the mathematical expectation, $\text{vec}(\mathbf{A})$ denotes the vectorization operator which stacks the columns of \mathbf{A} , $\text{tr}\{\cdot\}$ denotes the matrix trace, $\lceil \cdot \rceil$ denotes the ceiling operator and \mathbb{S}^1 denotes the unit circle. The matrix \mathbf{I}_n is the $n \times n$ identity matrix.

II. SPATIAL CHANNEL MODEL

First we review the spatial channel model proposed in [18]. Consider a MIMO system consisting of n_T transmit antennas located at positions \mathbf{u}_t , $t = 1, 2, \dots, n_T$ relative to the transmitter array origin, and n_R receive antennas located at positions \mathbf{v}_r , $r = 1, 2, \dots, n_R$ relative to the receiver array origin. $r_T \geq \max \|\mathbf{u}_t\|$ and $r_R \geq \max \|\mathbf{v}_r\|$ denote the radius of spheres that contain all the transmitter and receiver antennas, respectively. We assume that scatterers are distributed in the far field from the transmitter and receiver antennas and regions containing the transmit and receive antennas are distinct.

By taking into account physical aspects of scattering, the MIMO channel matrix \mathbf{H} can be decomposed into deterministic and random parts as [18]

$$\mathbf{H} = \mathbf{J}_R \mathbf{H}_S \mathbf{J}_T^\dagger, \quad (1)$$

where \mathbf{J}_R is the deterministic receiver configuration matrix,

$$\mathbf{J}_R = \begin{bmatrix} \mathcal{J}_{-N_R}(\mathbf{v}_1) & \cdots & \mathcal{J}_{N_R}(\mathbf{v}_1) \\ \mathcal{J}_{-N_R}(\mathbf{v}_2) & \cdots & \mathcal{J}_{N_R}(\mathbf{v}_2) \\ \vdots & \ddots & \vdots \\ \mathcal{J}_{-N_R}(\mathbf{v}_{n_R}) & \cdots & \mathcal{J}_{N_R}(\mathbf{v}_{n_R}) \end{bmatrix},$$

and \mathbf{J}_T is the deterministic transmitter configuration matrix,

$$\mathbf{J}_T = \begin{bmatrix} \mathcal{J}_{-N_T}(\mathbf{u}_1) & \cdots & \mathcal{J}_{N_T}(\mathbf{u}_1) \\ \mathcal{J}_{-N_T}(\mathbf{u}_2) & \cdots & \mathcal{J}_{N_T}(\mathbf{u}_2) \\ \vdots & \ddots & \vdots \\ \mathcal{J}_{-N_T}(\mathbf{u}_{n_T}) & \cdots & \mathcal{J}_{N_T}(\mathbf{u}_{n_T}) \end{bmatrix}.$$

$\mathcal{J}_n(\mathbf{w})$ is the spatial-to-mode function (SMF) which maps the antenna location \mathbf{w} to the n -th mode of the region. The form

which the SMF takes is related to the shape of the scatterer-free antenna region. For a circular region in 2-dimensional space, the SMF is given by a Bessel function of the first kind [18] and for a spherical region in 3-dimensional space, the SMF is given by a spherical Bessel function [19]. For a prism-shaped region in 3-dimensional space, the SMF is given by a prolate spheroidal function [20].

Here we consider the situation where the multipath is restricted to the azimuth plane only (2-D scattering environment), having no field components arriving at significant elevations. In this case, the SMF is given by

$$\mathcal{J}_n(\mathbf{w}) \triangleq J_n(k\|\mathbf{w}\|)e^{in(\phi_w - \pi/2)},$$

where $J_n(\cdot)$ is the Bessel function of integer order n , vector $\mathbf{w} \equiv (\|\mathbf{w}\|, \phi_w)$ in polar coordinates is the antenna location relative to the origin of the aperture, $k = 2\pi/\lambda$ is the wave number with λ being the wave length and $i = \sqrt{-1}$. \mathbf{J}_T is $n_T \times (2N_T + 1)$ and \mathbf{J}_R is $n_R \times (2N_R + 1)$, where $2N_T + 1$ and $2N_R + 1$ are the number of effective² communication modes at the transmit and receive regions, respectively. Note, N_T and N_R are defined by the size of the regions containing all the transmit and receive antennas, respectively [21]. In our case,

$$N_T = \left\lfloor \frac{ker_T}{\lambda} \right\rfloor \quad \text{and} \\ N_R = \left\lfloor \frac{ker_R}{\lambda} \right\rfloor,$$

where $e \approx 2.7183$.

Finally, \mathbf{H}_S is the $(2N_R + 1) \times (2N_T + 1)$ random complex scattering channel matrix with (ℓ, m) -th element given by

$$\{\mathbf{H}_S\}_{\ell, m} = \iint_{\mathbb{S}^1 \times \mathbb{S}^1} g(\phi, \varphi) e^{i(m - N_T - 1)\phi} e^{-i(\ell - N_R - 1)\varphi} d\phi d\varphi \quad (2)$$

representing the complex scattering gain between the $(m - N_T - 1)$ -th mode of the scatter-free transmit region and $(\ell - N_R - 1)$ -th mode of the scatter-free receiver region, where $g(\phi, \varphi)$ is the effective random complex scattering gain function for signals with angle-of-departure ϕ from the scatter-free transmitter region and angle-of-arrival φ at the scatter-free receiver region.

The channel matrix decomposition (1) separates the channel into three distinct regions of interest: the scatter-free region around the transmitter antenna array, the scatter-free region around the receiver antenna array and the complex random scattering environment which is the complement of the union of two antenna array regions. Consequently, the MIMO channel is decomposed into deterministic and random matrices, where deterministic portions \mathbf{J}_T and \mathbf{J}_R represent the physical configuration of the transmitter and the receiver antenna arrays, respectively, and the random portion represents the complex scattering environment between the transmitter and the receiver antenna regions. The reader is referred to [18] for more information regarding this spatial channel model.

²Although there are infinite number of modes excited by an antenna array, there are only finite number of modes $(2N + 1)$ which have sufficient power to carry information.

Note that the precoder design is based on this channel model, but the performance does not depend on this model (see Section VIII). That is, our design and simulations provide an independent confirmation of the validity and usefulness of this channel model.

A. Spatial Correlation

Suppose transmitter configuration matrix \mathbf{J}_T has the singular value decomposition (svd) $\mathbf{J}_T = \mathbf{U}_T \mathbf{\Lambda}_T \mathbf{V}_T^\dagger$ and receiver configuration matrix \mathbf{J}_R has the svd $\mathbf{J}_R = \mathbf{U}_R \mathbf{\Lambda}_R \mathbf{V}_R^\dagger$. Substituting svds of \mathbf{J}_T and \mathbf{J}_R in (1) and using the Kronecker product identity [22, page 180] $\text{vec}(\mathbf{A}\mathbf{X}\mathbf{B}) = (\mathbf{B}^T \otimes \mathbf{A}) \text{vec}(\mathbf{X})$, we obtain

$$\mathbf{h} = \mathbf{h}_{JS} (\mathbf{U}_R^T \otimes \mathbf{U}_T^\dagger), \quad (3)$$

where $\mathbf{h}_{JS} = (\text{vec}(\mathbf{H}_{JS}^T))^T$ with $\mathbf{H}_{JS} = \mathbf{\Lambda}_R \mathbf{V}_R^\dagger \mathbf{H}_S \mathbf{V}_T \mathbf{\Lambda}_T^\dagger$. Applying the same Kronecker product identity to $\text{vec}(\mathbf{H}_{JS}^T)$ yields $\mathbf{h}_{JS} = \mathbf{h}_S [(\mathbf{V}_R^* \mathbf{\Lambda}_R^T) \otimes (\mathbf{V}_T \mathbf{\Lambda}_T^\dagger)]$, where $\mathbf{h}_S = (\text{vec}(\mathbf{H}_S^T))^T$. Then the covariance matrix \mathbf{R}_H of the MIMO channel \mathbf{H} is given by

$$\mathbf{R}_H \triangleq E \left\{ \mathbf{h} \mathbf{h}^\dagger \right\}, \\ = (\mathbf{U}_R^* \otimes \mathbf{U}_T) \mathbf{R}_{JS} (\mathbf{U}_R^T \otimes \mathbf{U}_T^\dagger), \quad (4)$$

where $\mathbf{R}_{JS} = [(\mathbf{\Lambda}_R^* \mathbf{V}_R^T) \otimes (\mathbf{\Lambda}_T \mathbf{V}_T^\dagger)] \mathbf{R}_S [(\mathbf{V}_R^* \mathbf{\Lambda}_R^T) \otimes (\mathbf{V}_T \mathbf{\Lambda}_T^\dagger)]$ with $\mathbf{R}_S = E \left\{ \mathbf{h}_S \mathbf{h}_S^\dagger \right\}$.

In this work, our main objective is to design a linear precoder which compensates for any detrimental effects of non-ideal antenna placement/configuration on the performance of space-time block codes. Here we assume that the scattering environment surrounding the transmitter and the receiver regions is ‘‘rich’’³, i.e., $\mathbf{R}_S = \mathbf{I}$. This assumption yields the simplification

$$\mathbf{R}_{JS} = [(\mathbf{\Lambda}_R^* \mathbf{V}_R^T) \otimes (\mathbf{\Lambda}_T \mathbf{V}_T^\dagger)] [(\mathbf{V}_R^* \mathbf{\Lambda}_R^T) \otimes (\mathbf{V}_T \mathbf{\Lambda}_T^\dagger)] \quad (5a)$$

$$= (\mathbf{\Lambda}_R^* \mathbf{\Lambda}_R^T) \otimes (\mathbf{\Lambda}_T \mathbf{\Lambda}_T^\dagger), \quad (5b)$$

where (5b) follows from (5a) by matrix identity [22, page 180] $(\mathbf{A} \otimes \mathbf{C})(\mathbf{B} \otimes \mathbf{D}) = \mathbf{A}\mathbf{B} \otimes \mathbf{C}\mathbf{D}$, provided that the matrix products $\mathbf{A}\mathbf{B}$ and $\mathbf{C}\mathbf{D}$ exist, and unitary matrix properties $\mathbf{V}_R^\dagger \mathbf{V}_R = \mathbf{I}$ and $\mathbf{V}_T^\dagger \mathbf{V}_T = \mathbf{I}$. Substituting (5b) into (4) gives

$$\mathbf{R}_H = (\mathbf{U}_R^* \otimes \mathbf{U}_T) (\mathbf{R}_R \otimes \mathbf{R}_T) (\mathbf{U}_R^T \otimes \mathbf{U}_T^\dagger), \quad (6)$$

where

$$\mathbf{R}_T = \mathbf{\Lambda}_T \mathbf{\Lambda}_T^\dagger \quad (7)$$

and

$$\mathbf{R}_R = (\mathbf{\Lambda}_R \mathbf{\Lambda}_R^\dagger)^T. \quad (8)$$

Note that both \mathbf{R}_R and \mathbf{R}_T are diagonal matrices, where the diagonal of \mathbf{R}_R consists of squared singular values of \mathbf{J}_R (or eigen-values of $\mathbf{J}_R \mathbf{J}_R^\dagger$) and diagonal of \mathbf{R}_T consists of squared singular values of \mathbf{J}_T (or eigen-values of $\mathbf{J}_T \mathbf{J}_T^\dagger$).

³Even though precoders are derived for rich scattering channels, these precoders provide significant performance improvements in non rich scattering channel environments, see Section VII-C.

III. SYSTEM MODEL

At time instance k , the space time encoder at the transmitter takes a set of modulated symbols $\mathbf{C}(k) = \{c_1(k), c_2(k), \dots, c_K(k)\}$ and maps them onto an $n_T \times T$ code word matrix $\mathbf{S}_{\ell(k)} \in \mathcal{V}$ of space-time modulated constellation matrices set $\mathcal{V} = \{\mathbf{S}_1, \mathbf{S}_2, \dots, \mathbf{S}_L\}$, where T is the code length, $L = q^K$ and q is the size of the constellation from which $c_n(k)$, $n = 1, \dots, K$ are drawn. By setting $|c_n(k)| = 1/\sqrt{K}$, each code word matrix $\mathbf{S}_{\ell(k)}$ in \mathcal{V} will satisfy the property $\mathbf{S}_{\ell(k)} \mathbf{S}_{\ell(k)}^\dagger = \mathbf{I}_{n_T}$ for $\ell(k) = 1, 2, \dots, L$.

In this paper, we mainly focus on the space-time modulated constellations with the property

$$(\mathbf{S}_i - \mathbf{S}_j)(\mathbf{S}_i - \mathbf{S}_j)^\dagger = \beta_{i,j} \mathbf{I}_{n_T}, \forall i \neq j, \quad (9)$$

where $\beta_{i,j}$ is a scalar and $\mathbf{S}_i, \mathbf{S}_j \in \mathcal{V}$. Space-time orthogonal designs in [5] and some cyclic and dicyclic space-time modulated constellations in [7] are some examples which satisfy property (9) above.

A. Coherent Space-time Block Codes

Let \mathbf{s}_n be the n -th column of $\mathbf{S}_i = [\mathbf{s}_1, \mathbf{s}_2, \dots, \mathbf{s}_T] \in \mathcal{V}$. At the transmitter, each code vector \mathbf{s}_n is multiplied by a $n_T \times n_T$ fixed linear precoder matrix \mathbf{F}_c before transmitting out from n_T antennas. Assuming quasi-static fading, the signals received at n_R receiver antennas during T symbol periods can be expressed in matrix form as

$$\mathbf{Y}(k) = \sqrt{E_s} \mathbf{H} \mathbf{F}_c \mathbf{S}_{\ell(k)} + \mathbf{N}(k),$$

where E_s is the average transmitted signal energy per symbol period, $\mathbf{N}(k)$ is the $n_R \times T$ white Gaussian noise matrix in which elements are zero-mean independent Gaussian distributed random variables with variance $\sigma_n^2/2$ per dimension and \mathbf{H} is the $n_R \times n_T$ channel matrix. In this work, we use the channel decomposition (1) to represent the underlying MIMO channel and the elements of scattering channel matrix \mathbf{H}_S are modeled as zero-mean complex Gaussian random variables (Rayleigh fading).

For coherent STBC, we assume that the receiver has perfect channel state information (CSI) and transmitter has partial CSI (antenna placement details). At the receiver, the transmitted codeword is detected by applying the minimum Euclidian distance detection rule:

$$\begin{aligned} \hat{\mathbf{S}}_{\ell(k)} &= \arg \min_{\mathbf{S}_{\ell(k)} \in \mathcal{V}} \|\mathbf{y}(k) - \sqrt{E_s} \tilde{\mathbf{h}} \mathbf{S}_{\ell(k)}\|^2 \\ &= \arg \max_{\mathbf{S}_{\ell(k)} \in \mathcal{V}} \text{Re}\{\tilde{\mathbf{h}} \mathbf{S}_{\ell(k)} \mathbf{y}^\dagger(k)\}, \end{aligned} \quad (10)$$

where $\mathbf{y}(k) = (\text{vec}(\mathbf{Y}^T(k)))^T$, $\mathbf{S}_{\ell(k)} = \mathbf{I}_{n_R} \otimes \mathbf{S}_{\ell(k)}$ and $\tilde{\mathbf{h}} = (\text{vec}(\tilde{\mathbf{H}}^T))^T$ with $\tilde{\mathbf{H}} = \mathbf{H} \mathbf{F}_c$.

B. Differential Space-time Block Codes

In this scheme, codeword matrix $\mathbf{S}_{\ell(k)}$ is differentially encoded according to the rule

$$\mathbf{X}(k) = \mathbf{X}(k-1) \mathbf{S}_{\ell(k)}, \text{ for } k = 1, 2, \dots$$

with $\mathbf{X}(0) = \mathbf{I}_{n_T}$. Then, each encoded $\mathbf{X}(k)$ is multiplied by a $n_T \times n_T$ fixed linear precoder matrix \mathbf{F}_d before transmitting out from n_T transmit antennas. Assuming quasi-static fading, the signals received at n_R receiver antennas during n_T symbol periods can be expressed in matrix form as

$$\mathbf{Y}(k) = \sqrt{E_s} \mathbf{H} \mathbf{F}_d \mathbf{X}(k) + \mathbf{N}(k),$$

where $\mathbf{N}(k)$ is the $n_R \times n_T$ white Gaussian noise matrix in which elements are zero-mean independent Gaussian distributed random variables with variance $\sigma_n^2/2$ per complex dimension and \mathbf{H} is the $n_R \times n_T$ channel matrix, which is modeled using (1).

Assume that the scattering channel matrix \mathbf{H}_S remains constant during the reception of two consecutive received signal blocks $\mathbf{Y}(k-1)$ and $\mathbf{Y}(k)$, which can be expressed in vector (row) form as

$$\begin{aligned} \mathbf{y}(k-1) &= \sqrt{E_s} \mathbf{h} \mathbf{X}(k-1) + \mathbf{n}(k-1), \\ \mathbf{y}(k) &= \sqrt{E_s} \mathbf{h} \mathbf{X}(k) + \mathbf{n}(k), \\ &= \mathbf{y}(k-1) \mathbf{S}_{\ell(k)} + \mathbf{w}(k), \end{aligned} \quad (11)$$

where $\mathbf{y}(k) = (\text{vec}(\mathbf{Y}(k)^T))^T$, $\mathbf{X}(k) = \mathbf{I}_{n_R} \otimes (\mathbf{F}_d \mathbf{X}(k))$, $\mathbf{h} = (\text{vec}(\mathbf{H}^T))^T$, $\mathbf{n}(k) = (\text{vec}(\mathbf{N}(k)^T))^T$, $\mathbf{S}_{\ell(k)} = \mathbf{I}_{n_R} \otimes \mathbf{S}_{\ell(k)}$ and $\mathbf{w}(k) = \mathbf{n}(k) - \mathbf{n}(k-1) \mathbf{S}_{\ell(k)}$.

For differential STBC, we assume that receiver has no CSI whilst transmitter has partial CSI (antenna placement details). From (11), the transmitted code word matrix is detected differentially using the minimum Euclidian distance detection rule:

$$\begin{aligned} \hat{\mathbf{S}}_{\ell(k)} &= \arg \min_{\mathbf{S}_{\ell(k)} \in \mathcal{V}} \|\mathbf{y}(k) - \mathbf{y}(k-1) \mathbf{S}_{\ell(k)}\|^2 \\ &= \arg \max_{\mathbf{S}_{\ell(k)} \in \mathcal{V}} \text{Re}\{\mathbf{y}(k-1) \mathbf{S}_{\ell(k)} \mathbf{y}(k)^\dagger\}. \end{aligned}$$

IV. PROBLEM SETUP: COHERENT STBC

Assume that perfect CSI is available at the receiver and also maximum likelihood (ML) detection is employed at the receiver. Suppose codeword $\mathbf{S}_i \in \mathcal{V}$ is transmitted, but the ML-decoder (10) chooses codeword $\mathbf{S}_j \in \mathcal{V}$, then as shown in the Appendix I, the average pairwise error probability (PEP) is upper bounded by

$$P(\mathbf{S}_i \rightarrow \mathbf{S}_j) \leq \frac{1}{\left| \mathbf{I}_{n_T n_R} + \frac{\bar{\gamma}}{4} \mathbf{R}_H [\mathbf{I}_{n_R} \otimes \mathbf{S}_\Delta] \right|}, \quad (12)$$

where $\mathbf{S}_\Delta = \mathbf{F}_c (\mathbf{S}_i - \mathbf{S}_j) (\mathbf{S}_i - \mathbf{S}_j)^\dagger \mathbf{F}_c^\dagger$, $\mathbf{R}_H = E\{\mathbf{h}^\dagger \mathbf{h}\}$ with row vector $\mathbf{h} = (\text{vec}(\mathbf{H}^T))^T$ and $\bar{\gamma} = E_s/\sigma_n^2$ is the average symbol energy-to-noise ratio (SNR) at each receiver antenna. Substituting (6) in (12) and applying the property (9) associated with orthogonal space-time block codes we obtain

$$P(\mathbf{S}_i \rightarrow \mathbf{S}_j) \leq \frac{1}{\left| \mathbf{I}_{n_T n_R} + \frac{\bar{\gamma} \beta_{i,j}}{4} \mathbf{R}_{RT} [\mathbf{I}_{n_R} \otimes \mathbf{U}_T^\dagger \mathbf{F}_c \mathbf{F}_c^\dagger \mathbf{U}_T] \right|}, \quad (13)$$

where we have used the matrix determinant identity $|\mathbf{I} + \mathbf{A}\mathbf{B}| = |\mathbf{I} + \mathbf{B}\mathbf{A}|$ and let $\mathbf{R}_{RT} = \mathbf{R}_R \otimes \mathbf{R}_T$.

Optimization Problem 1: Find the optimum spatial precoder \mathbf{F}_c that minimizes the average PEP upper bound (13) for coherent STBC, subject to the transmit power constraint $\text{tr}\{\mathbf{F}_c\mathbf{F}_c^\dagger\} = n_T$, for given transmitter and receiver antenna configurations in a rich scattering environment.

A. Optimum Spatial Precoder: Coherent STBC

The linear precoder \mathbf{F}_c is designed by minimizing the maximum of all PEP upper bounds subject to the power constraint $\text{tr}\{\mathbf{F}_c\mathbf{F}_c^\dagger\} = n_T$. Alternatively, let

$$\mathbf{Q}_c = \frac{\bar{\gamma}\beta_{k,\ell}}{4}\mathbf{U}_T^\dagger\mathbf{F}_c\mathbf{F}_c^\dagger\mathbf{U}_T,$$

then the average PEP bound (13) becomes

$$P(\mathbf{S}_i \rightarrow \mathbf{S}_j) \leq \frac{1}{|\mathbf{I}_{n_T n_R} + [\mathbf{R}_R \otimes \mathbf{R}_T][\mathbf{I}_{n_R} \otimes \mathbf{Q}_c]|}, \quad (14)$$

and \mathbf{Q}_c must satisfy the power constraint $\text{tr}\{\mathbf{Q}_c\} = n_T\bar{\gamma}\beta_{k,\ell}/4$. Since $\log(\cdot)$ is a monotonically increasing function, the logarithm of the average PEP upper bound (14) is used as the objective function to minimize. Note that \mathbf{Q}_c in (14) is always positive semi-definite as $\mathbf{Q}_c = \mathbf{B}\mathbf{B}^\dagger$, with $\mathbf{B} = \sqrt{(\bar{\gamma}\beta_{k,\ell})/4}\mathbf{U}_T^\dagger\mathbf{F}_c$.

Now the optimum \mathbf{Q}_c is obtained by solving the optimization problem:

$$\begin{aligned} \min \quad & -\log|\mathbf{I}_{n_T n_R} + (\mathbf{R}_R \otimes \mathbf{R}_T)(\mathbf{I}_{n_R} \otimes \mathbf{Q}_c)| \\ \text{subject to} \quad & \mathbf{Q}_c \succeq 0, \text{tr}\{\mathbf{Q}_c\} = \frac{n_T\bar{\gamma}\beta}{4}, \end{aligned} \quad (15)$$

where $\beta = \min_{k \neq \ell} \{\beta_{k,\ell}\}$ over all possible codewords⁴. By applying Hadamard's inequality on $|\mathbf{I} + (\mathbf{R}_R \otimes \mathbf{R}_T)(\mathbf{I} \otimes \mathbf{Q}_c)|$ gives that this determinant is maximized when $(\mathbf{R}_R \otimes \mathbf{R}_T)(\mathbf{I} \otimes \mathbf{Q}_c)$ is diagonal [1]. Therefore \mathbf{Q}_c must be diagonal as \mathbf{R}_R and \mathbf{R}_T are both diagonal. Since $(\mathbf{R}_R \otimes \mathbf{R}_T)(\mathbf{I} \otimes \mathbf{Q}_c)$ is a positive semi-definite diagonal matrix with non-negative entries on its diagonal, $\mathbf{I} + (\mathbf{R}_R \otimes \mathbf{R}_T)(\mathbf{I} \otimes \mathbf{Q}_c)$ forms a positive definite matrix. As a result, the objective function of our optimization problem is convex [23, page 73]. Therefore the optimization problem (15) above is a convex minimization problem because the objective function and inequality constraints are convex and equality constraint is affine.

Let $q_i = [\mathbf{Q}_c]_{i,i}$, $t_i = [\mathbf{R}_T]_{i,i}$ and $r_j = [\mathbf{R}_R]_{j,j}$. Optimization problem (15) then reduces to finding $q_i > 0$ such that

$$\begin{aligned} \min \quad & -\sum_{j=1}^{n_R} \sum_{i=1}^{n_T} \log(1 + t_i q_i r_j) \\ \text{subject to} \quad & \mathbf{q} \succeq 0, \\ & \mathbf{1}^T \mathbf{q} = \frac{n_T\bar{\gamma}\beta}{4} \end{aligned} \quad (16)$$

where $\mathbf{q} = [q_1, q_2, \dots, q_{n_T}]^T$ and $\mathbf{1}$ denotes the vector of all ones.

Introducing Lagrange multipliers $\boldsymbol{\lambda}_c \in \mathbb{R}^{n_T}$ for the inequality constraints $-\mathbf{q} \preceq 0$ and $v_c \in \mathbb{R}$ for the equality constraint

⁴Setting $\beta = \min_{i \neq j} \{\beta_{i,j}\}$ will minimize the error probability of the dominant error event(s).

$\mathbf{1}^T \mathbf{q} = n_T\bar{\gamma}\beta/4$, we obtain the Karush-Kuhn-Tucker (K.K.T) conditions

$$\begin{aligned} \mathbf{q} \succeq 0, \quad \boldsymbol{\lambda}_c \succeq 0, \quad \mathbf{1}^T \mathbf{q} &= \frac{n_T\bar{\gamma}\beta}{4} \\ \lambda_i q_i &= 0, \quad i = 1, 2, \dots, n_T \\ -\sum_{j=1}^{n_R} \frac{r_j t_i}{1 + r_j t_i q_i} - \lambda_i + v_c &= 0, \quad i = 1, 2, \dots, n_T. \end{aligned} \quad (17)$$

λ_i in (17) can be eliminated since it acts as a slack variable⁵, giving new K.K.T conditions

$$\begin{aligned} \mathbf{q} \succeq 0, \quad \mathbf{1}^T \mathbf{q} &= \frac{n_T\bar{\gamma}\beta}{4} \\ q_i \left(v_c - \sum_{j=1}^{n_R} \frac{r_j t_i}{1 + r_j t_i q_i} \right) &= 0, \quad i = 1, \dots, n_T, \end{aligned} \quad (18a)$$

$$v_c \geq \sum_{j=1}^{n_R} \frac{r_j t_i}{1 + r_j t_i q_i}, \quad i = 1, \dots, n_T. \quad (18b)$$

For $n_R = 1$, the optimal solution to (18) is given by the classical ‘‘water-filling’’ solution found in information theory [1]. The optimal q_i for this case is given in Section IV-B. For $n_R > 1$, the main problem in finding the optimal q_i for given t_i and $r_j, j = 1, 2, \dots, n_R$ is the case that, there are multiple terms that involve q_i on (18a). Therefore we can view our optimization problem (16) as a *generalized water-filling* problem. In fact the optimum q_i for this optimization problem is given by the solution to a polynomial obtained from (18a). In Sections IV-C and IV-D, we provide closed form expressions for optimum q_i for $n_R = 2$ and 3 receiver antennas and a generalized method which gives optimum q_i for $n_R > 3$ is discussed in Section IV-E.

As shown above, the optimal \mathbf{Q}_c is diagonal with

$$\mathbf{Q}_c = \text{diag}\{q_1, q_2, \dots, q_{n_T}\},$$

and optimal spatial precoder \mathbf{F}_c is obtained by forming

$$\mathbf{F}_c = \sqrt{\frac{4}{\beta\bar{\gamma}}}\mathbf{U}_T\mathbf{Q}_c^{\frac{1}{2}}\mathbf{U}_n^\dagger,$$

where \mathbf{U}_n is any unitary matrix. In this work, we set $\mathbf{U}_n = \mathbf{I}_{n_T}$.

B. MISO Channel

Consider a MISO channel where we have n_T transmit antennas and a single receive antenna. The optimization problem involved in this case is similar to the water-filling problem in information theory, which has the optimal solution

$$q_i = \begin{cases} \frac{1}{v_c} - \frac{1}{t_i}, & v_c < t_i, \\ 0, & \text{otherwise,} \end{cases}$$

where the water-level $1/v_c$ is chosen to satisfy

$$\sum_{i=1}^{n_T} \max\left(0, \frac{1}{v_c} - \frac{1}{t_i}\right) = \frac{n_T\bar{\gamma}\beta}{4}.$$

⁵If $g(x) \leq v$ is a constraint inequality, then a variable λ with the property that $g(x) + \lambda = v$ is called a slack variable [23].

We now consider the case of n_T transmit antennas and $n_R = 2$ receive antennas. As shown in the Appendix II, the optimum q_i for this case is

$$q_i = \begin{cases} A + \sqrt{K}, & v_c < t_i(r_1 + r_2); \\ 0, & \text{otherwise,} \end{cases} \quad (19)$$

where v_c is chosen to satisfy

$$\sum_{i=1}^{n_T} \max\left(0, A + \sqrt{K}\right) = \frac{n_T \bar{\gamma} \beta}{4},$$

with

$$A = \frac{2r_1 r_2 t_i^2 - v_c t_i (r_1 + r_2)}{2v_c r_1 r_2 t_i^2} \quad \text{and} \\ K = \frac{v_c^2 t_i^2 (r_1 - r_2)^2 + 4r_1^2 r_2^2 t_i^4}{2v_c r_1 r_2 t_i^2}. \quad (20)$$

D. $n_T \times 3$ MIMO Channel

For the case of n_T transmit antennas and $n_R = 3$ receive antennas, the optimum q_i is given by

$$q_i = \begin{cases} -\frac{a_2}{3a_3} + S + T, & v_c < t_i(r_1 + r_2 + r_3); \\ 0, & \text{otherwise,} \end{cases} \quad (21)$$

where v_c is chosen to satisfy

$$\sum_{i=1}^{n_T} \max\left(0, -\frac{a_2}{3a_3} + S + T\right) = \frac{n_T \bar{\gamma} \beta}{4},$$

with

$$S + T = \left[R + \sqrt{Q^3 + R^2} \right]^{\frac{1}{3}} + \left[R - \sqrt{Q^3 + R^2} \right]^{\frac{1}{3}}, \\ Q = \frac{3a_1 a_3 - a_2^2}{9a_3^2}, \quad R = \frac{9a_1 a_2 a_3 - 27a_0 a_3^2 - 2a_2^3}{54a_3^3},$$

$a_3 = v_c r_1 r_2 r_3 t_i^3$, $a_2 = v_c t_i^2 (r_1 r_2 + r_1 r_3 + r_2 r_3) - 3r_1 r_2 r_3 t_i^3$, $a_1 = v_c t_i (r_1 + r_2 + r_3) - 2t_i^2 (r_1 r_2 + r_1 r_3 + r_2 r_3)$ and $a_0 = v_c - t_i (r_1 + r_2 + r_3)$. A sketch of the proof of (21) is given in the Appendix-III.

E. A Generalized Method

We now discuss a method which allows to find optimum solution to (16) for a system with n_T transmit and n_R receive antennas. The complementary slackness condition $\lambda_i q_i = 0$ for $i = 1, 2, \dots, n_T$ states that λ_i is zero unless the i -th inequality constraint is active at the optimum. Thus, from (18a) we have two cases: (i) $q_i = 0$ for $v_c > t_i \sum_{j=1}^{n_R} r_j$, (ii) $v_c = \sum_{j=1}^{n_R} r_j t_i / (1 + r_j t_i q_i)$ for $q_i > 0$ [23, page 243]. For the later case, the optimum q_i is found by evaluating the roots of n_R -th order polynomial in q_i , where the polynomial is obtained from $v_c = \sum_{j=1}^{n_R} r_j t_i / (1 + r_j t_i q_i)$. Since the objective function of the optimization problem (16) is convex for $q > 0$, there exist at least one positive root to the n_R -th order polynomial for $v_c < t_i \sum_{j=1}^{n_R} r_j$. In the case of multiple positive roots, the optimum q_i is the one which gives the minimum to the objective function of (16). In both cases, v_c is chosen to satisfy the power constraint $\mathbf{1}^T \mathbf{q} = n_T \bar{\gamma} \beta / 4$.

For the Differential STBC, we again use the average PEP upper bound to derive the optimum spatial precoder that reduces the effects of non-ideal antenna placement on the performance of differential STBC. Below shows the derivation of the average PEP upper bound.

Based on (11), the receiver will erroneously select \mathbf{S}_j when \mathbf{S}_i was actually sent as the k -th information matrix if

$$\| \mathbf{y}(k) - \mathbf{y}(k-1) \mathbf{S}_j \|^2 \leq \| \mathbf{y}(k) - \mathbf{y}(k-1) \mathbf{S}_i \|^2, \\ \mathbf{y}(k-1) \mathbf{D}_{i,j} \mathbf{y}^\dagger(k-1) \leq 2\text{Re}\{\mathbf{w}(k) \Delta_{i,j}^\dagger \mathbf{y}^\dagger(k-1)\}, \quad (22)$$

where $\Delta_{i,j} = \mathbf{S}_j - \mathbf{S}_i = \mathbf{I}_{n_R} \otimes (\mathbf{S}_j - \mathbf{S}_i)$ and $\mathbf{D}_{i,j} = \Delta_{i,j} \Delta_{i,j}^\dagger = \mathbf{I}_{n_R} \otimes ((\mathbf{S}_i - \mathbf{S}_j)(\mathbf{S}_i - \mathbf{S}_j)^\dagger)$. For given $\mathbf{y}(k-1)$, the term on the left hand side of (22) is a constant and the term on the right hand side is a Gaussian random variable. Let $u = 2\text{Re}\{\mathbf{w}(k) \Delta_{i,j}^\dagger \mathbf{y}^\dagger(k-1)\}$, then in the Appendix IV we have shown that u has the conditional mean

$$\bar{m}_{u|\mathbf{y}(k-1)} = E\{u | \mathbf{y}(k-1)\}, \\ = 2\text{Re}\left\{ \bar{m}_{\mathbf{n}(k-1)|\mathbf{y}(k-1)} (\mathbf{I} - \mathbf{S}_i \mathbf{S}_j^\dagger) \mathbf{y}^\dagger(k-1) \right\},$$

where $\bar{m}_{\mathbf{n}(k-1)|\mathbf{y}(k-1)} = \sigma_n^2 \mathbf{y}(k-1) (\mathcal{X}^\dagger(k-1) \mathbf{R}_H \mathcal{X}(k-1) + \sigma_n^2 \mathbf{I}_{n_T n_R})^{-1}$, and the conditional variance

$$\sigma_{u|\mathbf{y}(k-1)}^2 = E\left\{ \|u - \bar{m}_{u|\mathbf{y}(k-1)}\|^2 | \mathbf{y}(k-1) \right\}, \\ = 2\mathbf{y}(k-1) \Delta_{i,j} \\ \times \left(\sigma_n^2 \mathbf{I} + \mathbf{S}_i^\dagger \Sigma_{\mathbf{n}(k-1)|\mathbf{y}(k-1)} \mathbf{S}_i \right) \Delta_{i,j}^\dagger \mathbf{y}^\dagger(k-1),$$

where $\Sigma_{\mathbf{n}(k-1)|\mathbf{y}(k-1)} = \sigma_n^2 (\mathbf{I} - \sigma_n^2 (E_s \mathcal{X}^\dagger(k-1) \mathbf{R}_H \mathcal{X}(k-1) + \sigma_n^2 \mathbf{I})^{-1})$. Recall that \mathbf{R}_H in $\bar{m}_{\mathbf{n}(k-1)|\mathbf{y}(k-1)}$ and $\Sigma_{\mathbf{n}(k-1)|\mathbf{y}(k-1)}$ is the channel correlation matrix, defined by (4) and $\mathcal{X}(k) = \mathbf{I}_{n_R} \otimes (\mathbf{F}_d \mathbf{X}(k))$.

Let $d_{i,j}^2 = \mathbf{y}(k-1) \mathbf{D}_{i,j} \mathbf{y}^\dagger(k-1)$. Based on (22), the PEP condition on received signal $\mathbf{y}(k-1)$ is given by

$$P(\mathbf{S}_i \rightarrow \mathbf{S}_j | \mathbf{y}(k-1)) = \Pr(U > d_{i,j}^2), \\ = \int_{d_{i,j}^2}^{\infty} \frac{1}{\sqrt{2\pi}\sigma} \exp\left(-\frac{(u - \bar{m})^2}{2\sigma^2}\right) du, \\ = Q\left(\frac{d_{i,j}^2 - \bar{m}}{\sigma}\right). \quad (23)$$

In order to obtain unconditional PEP, we need to average (23) with respect to the distribution of $\mathbf{y}(k-1)$. Unlike in the coherent STBC case, finding unconditional PEP from (23) poses a much harder problem due to the non-zero $\bar{m}_{u|\mathbf{y}(k-1)}$ and complicated $\sigma_{u|\mathbf{y}(k-1)}^2$. However, at asymptotically high SNRs (i.e., keeping E_s constant and $\sigma_n^2 \rightarrow 0$) the conditional mean and the conditional variance of u reduce to $\bar{m}_{u|\mathbf{y}(k-1)} = 0$ and $\sigma_{u|\mathbf{y}(k-1)}^2 = 4\sigma_n^2 d_{i,j}^2$, respectively. As shown in the Appendix V, the average PEP can be upper bounded by

$$P(\mathbf{S}_i \rightarrow \mathbf{S}_j) \leq \frac{1}{2} \frac{1}{\left| \mathbf{I} + \frac{1}{8} \left(\bar{\gamma} \mathcal{X}(k-1)^\dagger \mathbf{R}_H \mathcal{X}(k-1) + \mathbf{I}_{n_T n_R} \right) \mathbf{D}_{i,j} \right|}, \quad (24)$$

where $\bar{\gamma} = E_s/\sigma_n^2$ is the average SNR at each receiver antenna. As for the coherent STBC case, we mainly focus on the space-time modulated constellations with the property (9). Furthermore, similar to [7, 8] we assume that code length $T = n_T$. Under this assumption, each code word matrix \mathbf{S}_i in \mathcal{V} will satisfy the unitary property $\mathbf{S}_i \mathbf{S}_i^\dagger = \mathbf{I}$ and $\mathbf{S}_i^\dagger \mathbf{S}_i = \mathbf{I}$ for $i = 1, 2, \dots, L$. As a result, $\mathbf{X}(k)$ will also satisfy the unitary property $\mathbf{X}(k) \mathbf{X}^\dagger(k) = \mathbf{I}$ and $\mathbf{X}^\dagger(k) \mathbf{X}(k) = \mathbf{I}$ for $k = 0, 1, 2, \dots$. Applying (9) on (24) and then using the unitary property of $\mathbf{X}(k-1)$ and the determinant identity $|\mathbf{I} + \mathbf{A}\mathbf{B}| = |\mathbf{I} + \mathbf{B}\mathbf{A}|$, after straight forward manipulations, we can simplify the PEP upper bound (24) to

$$P(\mathbf{S}_i \rightarrow \mathbf{S}_j) \leq \frac{1}{2} \frac{\left(\frac{8+\beta_{i,j}}{8}\right)^{-n_T n_R}}{\left|\mathbf{I} + \frac{\beta_{i,j} \bar{\gamma}}{(8+\beta_{i,j})} \mathbf{R}_H (\mathbf{I}_{n_R} \otimes \mathbf{F}_d \mathbf{F}_d^\dagger)\right|}. \quad (25)$$

As before, we assume that the scattering environment surrounding the transmitter and receiver antenna arrays is isotropic. Then, substitution of (6) in (25) gives

$$P(\mathbf{S}_i \rightarrow \mathbf{S}_j) \leq \frac{1}{2} \frac{\left(\frac{8+\beta_{i,j}}{8}\right)^{-n_T n_R}}{\left|\mathbf{I} + \frac{\beta_{i,j} \bar{\gamma}}{(8+\beta_{i,j})} (\mathbf{R}_R \otimes \mathbf{R}_T) (\mathbf{I}_{n_R} \otimes \mathbf{U}_T^\dagger \mathbf{F}_d \mathbf{F}_d^\dagger \mathbf{U}_T)\right|}, \quad (26)$$

where \mathbf{R}_T and \mathbf{R}_R are defined by (7) and (8), respectively. The optimization problem for differential STBC case can now be stated as follows:

Optimization Problem 2: Find the optimum spatial precoder \mathbf{F}_d that minimizes the average PEP upper bound (26) for differential STBC, subject to the transmit power constraint $\text{tr}\{\mathbf{F}_d \mathbf{F}_d^\dagger\} = n_T$, for given transmitter and receiver antenna configurations in a rich scattering environment.

A. Optimum Spatial Precoder: Differential STBC

Similar to the coherent STBC case, the optimum spatial precoder \mathbf{F}_d for differential STBC is obtained by minimizing the maximum of all PEP upper bounds subject to the power constraint $\text{tr}\{\mathbf{F}_d \mathbf{F}_d^\dagger\} = n_T$. Let

$$\mathbf{P}_d = \frac{\beta_{i,j} \bar{\gamma}}{(8 + \beta_{i,j})} \mathbf{U}_T^\dagger \mathbf{F}_d \mathbf{F}_d^\dagger \mathbf{U}_T.$$

The optimum \mathbf{P}_d (hence the optimum \mathbf{F}_d) is then obtained by solving the optimization problem

$$\begin{aligned} \min \quad & -\log |\mathbf{I} + (\mathbf{R}_R \otimes \mathbf{R}_T) (\mathbf{I}_{n_R} \otimes \mathbf{P}_d)| \\ \text{subject to} \quad & \mathbf{P}_d \succeq 0, \text{tr}\{\mathbf{P}_d\} = \frac{\beta_{i,j} \bar{\gamma} n_T}{(8 + \beta_{i,j})}. \end{aligned}$$

The above optimization problem is identical to the optimization problem derived for coherent STBC, except a different scalar for the equality constraint. Therefore, following Section IV-A, here we present the final optimization problem and solutions to it without detail derivations.

Following Section IV-A, we can show that the optimum \mathbf{P}_d is diagonal and diagonal entries of \mathbf{P}_d are found by solving the optimization problem

$$\begin{aligned} \min \quad & -\sum_{j=1}^{n_R} \sum_{i=1}^{n_T} \log(1 + t_i p_i r_j) \\ \text{subject to} \quad & \mathbf{p} \succeq 0, \\ & \mathbf{1}^T \mathbf{p} = \frac{\beta \bar{\gamma} n_T}{(8 + \beta)} \end{aligned} \quad (27)$$

where $\beta = \min_{i \neq j} \{\beta_{i,j}\}$ over all possible codewords, $p_i = [\mathbf{P}_d]_{i,i}$, $t_i = [\mathbf{R}_T]_{i,i}$, $r_j = [\mathbf{R}_R]_{j,j}$ and $\mathbf{p} = [p_1, p_2, \dots, p_{n_T}]^T$. The linear spatial precoder \mathbf{F}_d is obtained by forming

$$\mathbf{F}_d = \sqrt{\frac{8 + \beta}{\beta \bar{\gamma}}} \mathbf{U}_T \mathbf{P}_d^{\frac{1}{2}} \mathbf{U}_n^\dagger,$$

where $\mathbf{P}_d = \text{diag}\{p_1, p_2, \dots, p_{n_T}\}$ and \mathbf{U}_n is any unitary matrix. Similar to coherent STBC case, when $n_R = 1$, the optimum power loading strategy is identical to the ‘‘water-filling’’ in information theory. When $n_R > 1$, a *generalized water-filling* strategy gives the optimum \mathbf{P}_d . Following Sections give the optimum p_i for (27) for $n_R = 1, 2, 3$ receive antennas. For other cases, the the generalized method discussed in Section IV-E can be directly applied to obtain the optimum p_i for (27).

B. MISO Channel

The optimization problem involved in this case is similar to the water-filling problem in information theory, which has the optimal solution

$$p_i = \begin{cases} \frac{1}{v_d} - \frac{1}{t_i}, & v_d < t_i, \\ 0, & \text{otherwise,} \end{cases} \quad (28)$$

where the water-level $1/v_d$ is chosen to satisfy

$$\sum_{i=1}^{n_T} \max\left(0, \frac{1}{v_d} - \frac{1}{t_i}\right) = \frac{\bar{\gamma} \beta n_T}{8 + \beta}.$$

C. $n_T \times 2$ MIMO Channel

The optimum p_i for this case is

$$p_i = \begin{cases} A + \sqrt{K}, & v_d < t_i(r_1 + r_2); \\ 0, & \text{otherwise,} \end{cases}$$

where v is chosen to satisfy

$$\sum_{i=1}^{n_T} \max\left(0, A + \sqrt{K}\right) = \frac{\bar{\gamma} \beta n_T}{8 + \beta}$$

with

$$A = \frac{2r_1 r_2 t_i^2 - v_d t_i (r_1 + r_2)}{2v_d r_1 r_2 t_i^2},$$

and

$$K = \frac{v_d^2 t_i^2 (r_1 - r_2)^2 + 4r_1^2 r_2^2 t_i^4}{2v_d r_1 r_2 t_i^2}.$$

TABLE I

TRANSMIT ANTENNA CONFIGURATION DETAILS CORRESPONDING TO WATER-FILLING SCENARIOS CONSIDERED IN FIG. 1.

Antenna Configuration	Tx aperture radius	Num. of modes	rank($\mathbf{J}_T \mathbf{J}_T^\dagger$)
2-Tx	0.1λ	3	2
3-Tx UCA	0.115λ	3	3
3-Tx ULA	0.2λ	5	3
4-Tx UCA	0.142λ	5	4
4-Tx ULA	0.3λ	7	4

D. $n_T \times 3$ MIMO Channel

For the case of n_T transmit antennas and $n_R = 3$ receive antennas, the optimum p_i is given by

$$p_i = \begin{cases} -\frac{z_2}{3z_3} + Z, & v_d < t_i(r_1 + r_2 + r_3); \\ 0, & \text{otherwise,} \end{cases}$$

where v_d is chosen to satisfy

$$\sum_{i=1}^{n_T} \max\left(0, -\frac{z_2}{3z_3} + Z\right) = \frac{\bar{\gamma}\beta n_T}{8 + \beta},$$

with

$$Z = \left[Z_2 + \sqrt{Z_1^3 + Z_2^2} \right]^{\frac{1}{3}} + \left[Z_2 - \sqrt{Z_1^3 + Z_2^2} \right]^{\frac{1}{3}},$$

$$Z_1 = \frac{3z_1z_3 - z_2^2}{9z_3^2}, \quad Z_2 = \frac{9z_1z_2z_3 - 27z_0z_3^2 - 2z_2^3}{54z_3^3},$$

$$z_3 = v_d r_1 r_2 r_3 t_i^3, \quad z_2 = v_d t_i^2 (r_1 r_2 + r_1 r_3 + r_2 r_3) - 3r_1 r_2 r_3 t_i^3,$$

$$z_1 = v_d t_i (r_1 + r_2 + r_3) - 2t_i^2 (r_1 r_2 + r_1 r_3 + r_2 r_3) \quad \text{and} \quad z_0 = v_d - t_i (r_1 + r_2 + r_3).$$

E. Spatially Uncorrelated Receive Antennas

If n_R receive antennas are placed ideally within the receiver region such that the spatial correlation between antenna elements is zero (i.e., $\mathbf{J}_R^\dagger \mathbf{J}_R = \mathbf{I}$), then the objective function in (27) reduces to a single summation and the optimum p_i is given by the water-filling solution (28) obtained for the MISO channel. This is not to say that such an ideal placement is possible even approximately. A similar result holds for the coherent STBC case.

VI. SIMULATION RESULTS: COHERENT STBC

In this section, we will illustrate the performance improvements obtained from coherent STBC when the spatial precoder \mathbf{F}_c derived in Section-IV-A is used. In particular, the performance is evaluated for small antenna separations and different antenna geometries at the transmitter and receiver antenna arrays, assuming an isotropic scattering environment (independent and identically distributed entries in scattering channel matrix \mathbf{H}_S). In our simulations we use the rate-1 space-time modulated constellation constructed in [5] from orthogonal designs for two transmit antennas. Also use the rate 3/4 STBC code for $n_T = 3, 4$ transmit antennas given in [5]. Modulated symbols $c(k)$ are drawn from the normalized QPSK alphabet $\{\pm 1/\sqrt{2} \pm i/\sqrt{2}\}$.

A. MISO Channels

First we illustrate the water-filling concept for $n_T = 2, 3$ and 4 transmit antennas, where the transmit antennas are placed in uniform circular array (UCA) and uniform linear array (ULA) configurations⁶ with 0.2λ minimum separation between two adjacent antenna elements. For each transmit antenna configuration we consider, Table-I lists the radius of the transmit aperture, number of effective communication

⁶This precoder can be applied to any arbitrary antenna configuration.

modes⁷[18] in the transmit region and the rank of the transmit side spatial correlation matrix $\mathbf{J}_T \mathbf{J}_T^\dagger$. Note that, in all spatial scenarios, we ensure that $\mathbf{J}_T \mathbf{J}_T^\dagger$ is full rank in order that the average PEP upper bound (12) to hold.

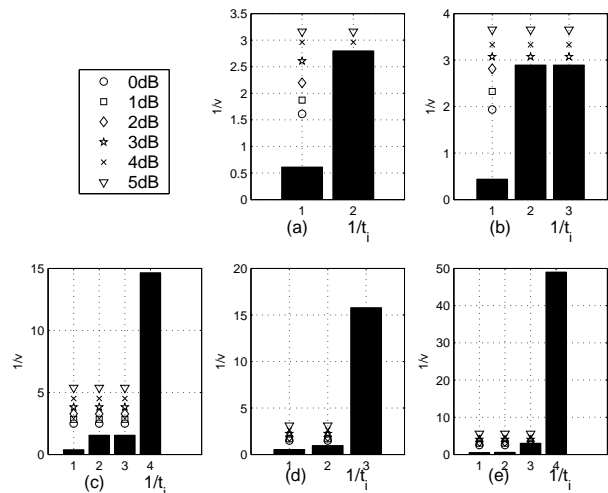


Fig. 1. Water level ($1/v_c$) for various SNRs for a MISO system. (a) $n_T = 2$, (b) $n_T = 3$ - UCA, (c) $n_T = 4$ - UCA, (d) $n_T = 3$ - ULA and (e) $n_T = 4$ - ULA for 0.2λ minimum separation between two adjacent transmit antennas.

Fig. 1 shows the water levels for various SNRs. For a given SNR, the optimal power value q_i is the difference between water-level $1/v_c$ and base level $1/t_i$, whenever the difference is positive; it is zero otherwise. Note that, with this spatial precoder, the diversity order of the system is determined by the number of non-zero q_i 's. It is observed that at low SNRs, only one q_i is non-zero for $n_T = 2$ and 3-UCA cases. In these cases, all the available power is assigned to the highest eigen-mode of $\mathbf{J}_T \mathbf{J}_T^\dagger$ (or to the single dominant eigen-channel of \mathbf{H}) and the system is operating in eigen-beamforming mode. With other cases, Fig. 1(c), (d) and (e), systems are operating in between eigen-beam forming and full diversity for small SNRs as well as moderate SNRs. In these cases, the spatial precoder assigns more power to the higher eigen-modes of $\mathbf{J}_T \mathbf{J}_T^\dagger$ (or to dominant eigen-channels of \mathbf{H}) and less power to the weaker eigen-modes (or to less dominant eigen-channels of \mathbf{H}).

⁷The set of modes form a basis of functions for representing a multipath wave field.

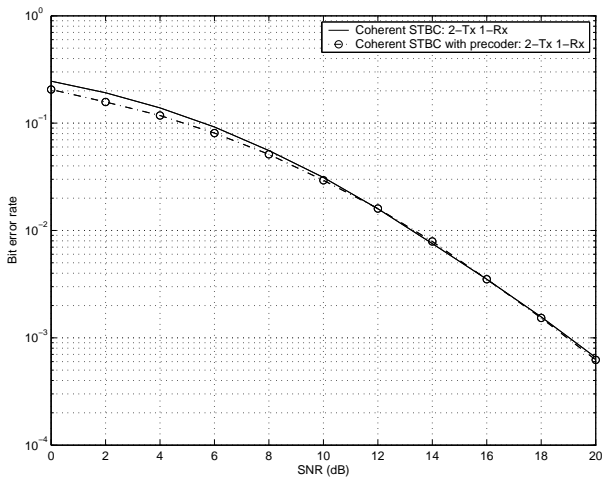


Fig. 2. Performance of spatial precoder with two transmit and one receive antennas for 0.2λ separation between two transmit antenna elements: rate-1 coherent STBC.

Fig. 2 illustrates the BER performance of the rate 1 STBC with and without spatial precoder for $n_T = 2$. It can be observed that at very low SNRs, we obtain a pre-coding gain of about 1.5dB. In fact, at very low SNRs, the optimum scheme is equivalent to eigen-beam forming. However, as the SNR increases, the precoder becomes redundant and the optimum scheme approaches STBC, where it operates in full diversity. This corroborates the claim that the 2×1 STBC has good resistance against the spatially correlated fading at high SNRs as shown in [24].

BER performance results for 3-Tx UCA, ULA and 4-Tx UCA, ULA antenna configurations are shown in Fig. 3 and 4, respectively for rate 3/4 STBCs. For 3-Tx UCA, the results obtained are similar to the results of $n_T = 2$ case above. In this case, at low SNRs, the system operates in eigen beam-forming mode and at high SNRs, it is operating in full diversity mode as shown in Fig. 1(b). For the other three cases, it is observed that the optimum scheme provides a clear performance advantage over the STBC only system for all SNRs concerned. For example, at 0.01 bit-error-rate, we obtain a precoding gain of about 1dB. However, these systems operate in between eigen beam-forming and full diversity as the precoder assigns zero powers to some of the transmit diversity branches of the channel. As before, at higher SNRs, the system operates in full diversity and the optimum scheme approaches STBC.

In all cases, at high SNRs we observed that ULA antenna configuration provides better performance than UCA antenna configuration when the spatial precoder is used. This is because, the number of effective communication modes in the transmit region is higher for the ULA case (large aperture radius of ULA, c.f. Table I) than the UCA case and the spatial precoder efficiently activates the modes in the transmit region of ULA. This observation suggests that our precoding scheme gives scope for improvement of ULA performance at high SNR.

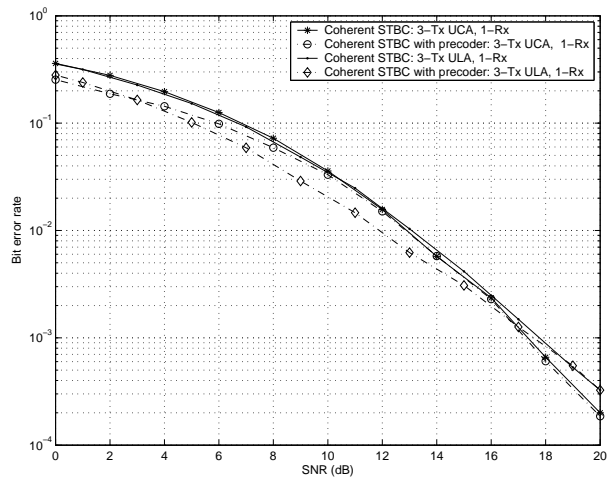


Fig. 3. Performance of spatial precoder with three transmit and one receive antennas for 0.2λ minimum separation between two adjacent transmit antennas for UCA and ULA antenna configurations: rate-3/4 coherent STBC.

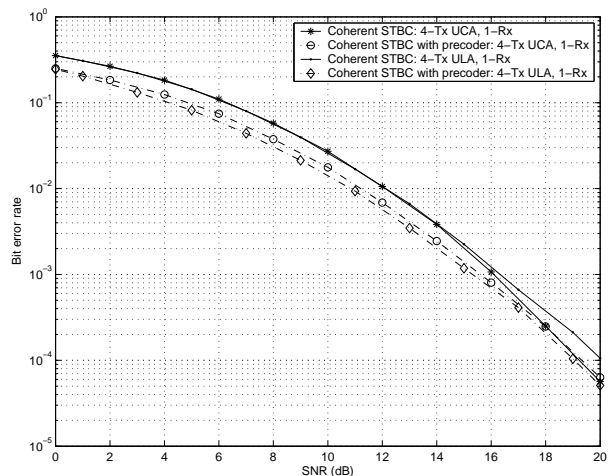


Fig. 4. Performance of spatial precoder with four transmit and one receive antennas for 0.2λ minimum separation between two adjacent transmit antennas for UCA and ULA antenna configurations: rate-3/4 coherent STBC.

B. MIMO Channels

We now examine the performance of the spatial precoder for multiple transmit and multiple receive antennas. For example, we consider $n_T = 2, 3$ transmit antennas and $n_R = 2$ receive antennas. In all cases, two receiver antennas are placed λ apart, which gives negligible effects on the performance due to antenna spacing. As before, the minimum separation between two adjacent transmit antennas is set to 0.2λ . Note that this situation reasonably models the uplink of a mobile communication system. For each case, the optimum q_i is calculated using (19). Fig. 5 illustrates the BER performance results for 2-transmit, 2-receive antennas for rate 1 STBC and Fig. 6 illustrates the BER performance results for 3-transmit, 2-receive antennas for rate 3/4 STBC. Performance results obtained here are similar to that of MISO cases above.

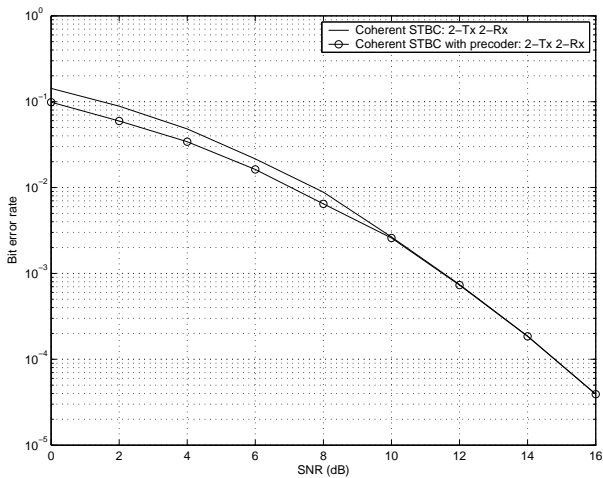


Fig. 5. Performance of spatial precoder with two transmit and one receive antennas: receive antenna separation λ and minimum transmit antenna separation 0.2λ for UCA and ULA antenna configurations: rate-3/4 coherent STBC.

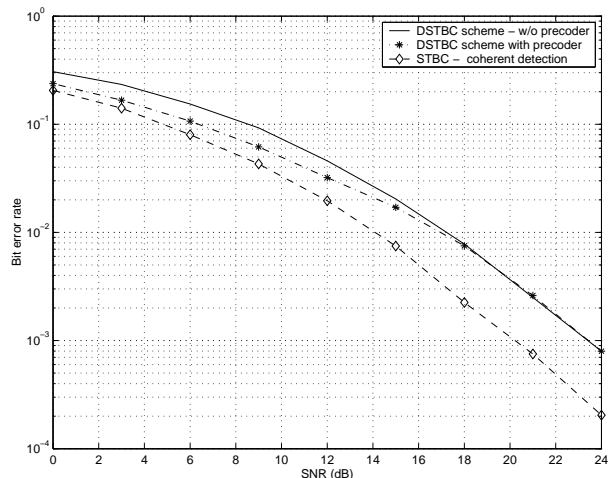


Fig. 7. Performance of spatial precoder with two transmit and one receive antennas for 0.1λ separation between two transmit antennas: rate-1 differential STBC.

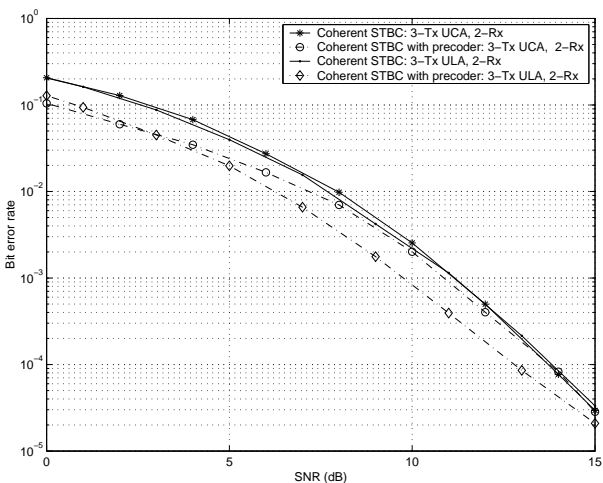


Fig. 6. Performance of spatial precoder with three transmit and two receive antennas: receive antenna separation λ and minimum transmit antenna separation 0.2λ for UCA and ULA antenna configurations: rate-3/4 coherent STBC.

VII. SIMULATION RESULTS: DIFFERENTIAL STBC

We now demonstrate the performance improvements obtained from differential space time block coded systems when the spatial precoder derived in Section V-A is applied. As before, the performance of differential space-time coded systems is investigated for small antenna separations and different antenna geometries assuming a rich scattering environment surrounding the transmit and receive antenna arrays (i.e., i.i.d entries in \mathbf{H}_S). We use the rate-1 space-time modulated constellations constructed in [5] from orthogonal designs for two and four transmit antennas. Normalized QPSK alphabet $\{\pm 1/\sqrt{2} \pm i/\sqrt{2}\}$ and normalized BPSK alphabet $\{\pm 1/\sqrt{2}\}$ are used with two and four transmit antenna STBC, respectively.

A. MISO Channel

Fig. 7 illustrates the BER performance of the differential STBC with and without spatial precoder when $n_T = 2$. Also shown for comparison is the BER performance of the STBC when coherent detection is employed at the receiver. In all cases, two transmit antennas are placed 0.1λ distance apart. It can be seen that at the BER of 0.05, the performance of the precoded system is 1.25dB better than that of the non-precoded differential orthogonal space-time coded system and 1.75dB away from the coherent detection case. However at high SNRs, the precoder becomes redundant and the optimum scheme approaches differential STBC.

BER performance results for 4-Tx UCA and 4-Tx ULA antenna configurations are shown in Fig. 8 and 9, respectively. For both antenna configurations, the minimum separation between two adjacent antenna elements is set to 0.2λ , corresponding to aperture radii 0.142λ and 0.3λ for UCA and ULA antenna configurations, respectively. Simulation results show that the BER performance of the optimum scheme is better than that of the differential STBC system for both antenna configurations. For example, at 10^{-2} BER, we obtain precoding gains of about 1dB and 1.5dB with UCA and ULA antenna configurations, respectively. In comparison with the coherent detection at the receiver, BER performance of the optimum scheme is 2dB and 1.5dB away for UCA and ULA antenna configurations, respectively.

B. MIMO Channel

We now examine the performance of the proposed optimum scheme for multiple transmit and multiple receive antennas. As an example, we consider a MIMO system consisting of $n_T = 2$ transmit antennas and $n_R = 2$ receive antennas. The two receiver antennas are placed λ apart, which gives minimum effect on the performance due to antenna spacing at the receiver antenna array, and the two transmit antennas are placed 0.1λ distance apart. Note that this situation reasonably models the uplink of a mobile communication system. Fig.

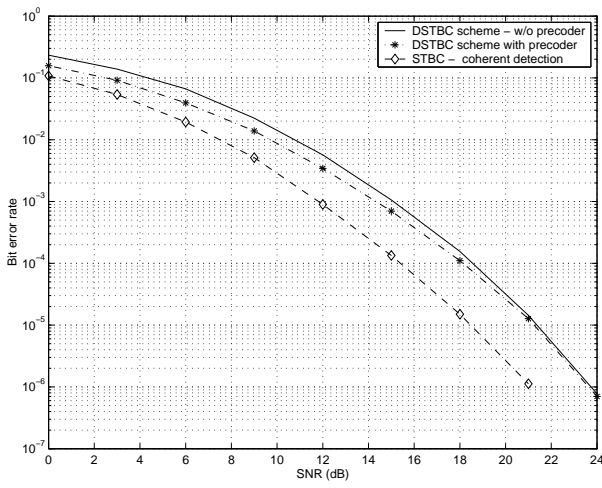


Fig. 8. Performance of spatial precoder with four transmit and one receive antennas for 0.2λ minimum separation between two adjacent transmit antennas; UCA transmit antenna configuration: rate-1 differential STBC.

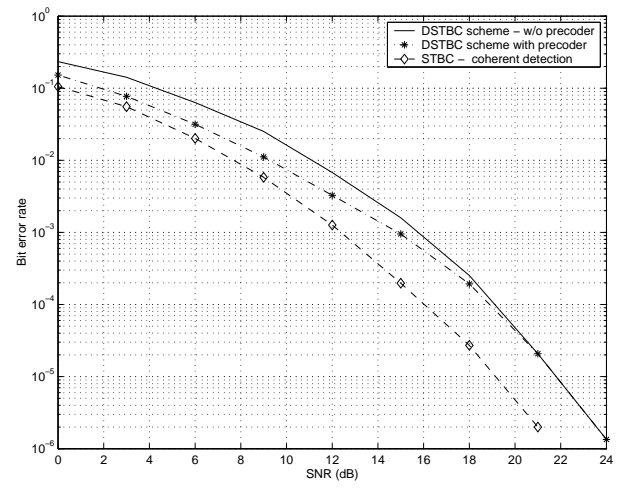


Fig. 10. Performance of spatial precoder with two transmit and two receive antennas. Transmit antenna separation 0.1λ and receive antenna separation λ ; rate-1 differential STBC.

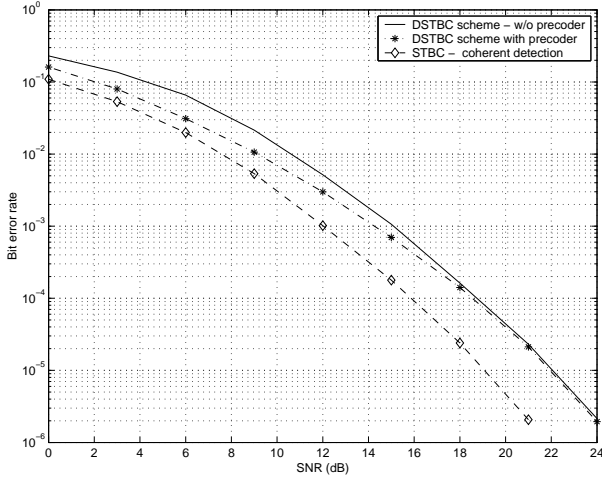


Fig. 9. Performance of spatial precoder with four transmit and one receive antennas for 0.2λ minimum separation between two adjacent transmit antennas; ULA transmit antenna configuration: rate-1 differential STBC.

10 shows the performance of the optimum scheme with two transmit and two receive antennas. Performance results obtained here are similar to that of MISO cases considered above.

Note the objective function of D-STBC optimization problem is derived for high SNR. However, from our simulation results, we observed that proposed precoding scheme also gives good performance at low SNRs.

C. Effects of Non-isotropic Scattering

In practise, wireless channels experience non-isotropic scattering (limited angular spread about a mean angle of departure/arrival) both at the transmitter and the receiver antenna arrays. We now investigate the effects of non-isotropic scattering on the BER performance of differential STBC when the spatial precoding scheme derived in Section V-A is used.

First we derive expressions for correlation between different communication modes at the transmitter and receiver aper-

tures. Using (2), we define the modal correlation between complex scattering gains as

$$\gamma_{m,m'}^{\ell,\ell'} \triangleq E \left\{ \{ \mathbf{H}_S \}_{\ell,m} \{ \mathbf{H}_S \}_{\ell',m'}^* \right\}.$$

Assume that the scattering from one direction is independent of that from another direction for both the receiver and the transmitter apertures. Then the second order statistics of the scattering gain function $g(\phi, \varphi)$ can be defined as

$$E \{ g(\phi, \varphi) g^*(\phi', \varphi') \} \triangleq G(\phi, \varphi) \delta(\phi - \phi') \delta(\varphi - \varphi'),$$

where $G(\phi, \varphi) = E \{ |g(\phi, \varphi)|^2 \}$ with normalization $\iint G(\phi, \varphi) d\phi d\varphi = 1$. With the above assumption, the modal correlation coefficient, $\gamma_{m,m'}^{\ell,\ell'}$ can be simplified to

$$\gamma_{m,m'}^{\ell,\ell'} = \iint_{\mathbb{S}^1 \times \mathbb{S}^1} G(\phi, \varphi) e^{-i(\ell-\ell')\varphi} e^{i(m-m')\phi} d\phi d\varphi.$$

Then the correlation between ℓ -th and ℓ' -th modes at the receiver region due to the m -th mode at the transmitter region is given by

$$\gamma^{\ell,\ell'} = \int_{\mathbb{S}^1} \mathcal{P}_{Rx}(\varphi) e^{-i(\ell-\ell')\varphi} d\varphi, \quad \forall m, \quad (29)$$

where $\mathcal{P}_{Rx}(\varphi) = \int G(\phi, \varphi) d\phi$ is the normalized azimuth power distribution (APD) of the scatterers surrounding the receiver antenna region. Here we see that modal correlation at the receiver is independent of the mode selected from transmitter region.

Similarly, we can write the correlation between m -th and m' -th modes at the transmitter region due to the ℓ -th mode at the receiver region as

$$\gamma_{m,m'} = \int_{\mathbb{S}^1} \mathcal{P}_{Tx}(\phi) e^{i(m-m')\phi} d\phi, \quad \forall \ell, \quad (30)$$

where $\mathcal{P}_{Tx}(\phi) = \int G(\phi, \varphi) d\varphi$ is the normalized azimuth power distribution at the transmitter region. As for the receiver modal correlation, we can observe that modal correlation at the transmitter is independent of the mode selected from receiver

region. Note that, azimuth power distributions $\mathcal{P}_{R_x}(\varphi)$ and $\mathcal{P}_{T_x}(\phi)$ can be modeled using all common power distributions such as uniform-limited [25], Gaussian [26], Laplacian [27], $\cos^{2p} \phi$ distribution [25], etc.

Denoting the p -th column of scattering matrix \mathbf{H}_S as $\mathbf{H}_{S,p}$, the $(2N_R + 1) \times (2N_R + 1)$ receiver modal correlation matrix can be defined as

$$\mathbf{M}_R \triangleq E \left\{ \mathbf{H}_{S,p} \mathbf{H}_{S,p}^\dagger \right\},$$

where (ℓ, ℓ') -th element of \mathbf{M}_R is given by (29) above. Similarly, the transmitter modal correlation matrix can be defined as

$$\mathbf{M}_T \triangleq E \left\{ \mathbf{H}_{S,q}^\dagger \mathbf{H}_{S,q} \right\},$$

where $\mathbf{H}_{S,q}$ is the q -th row of \mathbf{H}_S . (m, m') -th element of \mathbf{M}_T is given by (30) and \mathbf{M}_T is a $(2N_T + 1) \times (2N_T + 1)$ matrix.

1) *Kronecker Model as a Special Case:* The correlation between two distinct modal pairs can be written as the product of corresponding modal correlation at the transmitter and the modal correlation at the receiver, i.e.,

$$\gamma_{m,m'}^{\ell,\ell'} = \gamma_{m,m'}^{\ell,\ell'} \gamma_{m,m'}. \quad (31)$$

Facilitated by (31), we write the covariance matrix of the scattering channel \mathbf{H}_S as the Kronecker product between the receiver modal correlation matrix and the transmitter modal correlation matrix,

$$\mathbf{R}_S = E \left\{ \mathbf{h}_S^\dagger \mathbf{h}_S \right\} = \mathbf{M}_R \otimes \mathbf{M}_T. \quad (32)$$

Note that (31) holds only for class of scattering environments where the power spectral density of modal correlation function satisfies [28, 29]

$$G(\phi, \varphi) = \mathcal{P}_{T_x}(\phi) \mathcal{P}_{R_x}(\varphi). \quad (33)$$

Note that, (33) is the necessary condition in which a channel must satisfy in order for (32) to hold .

Assuming \mathbf{R}_S is a positive definite matrix, a channel realization of the scattering channel \mathbf{H}_S can be generated by

$$\text{vec}(\mathbf{H}_S) = \mathbf{R}_S^{1/2} \text{vec}(\mathbf{W}_S), \quad (34)$$

where $\mathbf{R}_S^{1/2}$ is the positive definite matrix square root [22] of \mathbf{R}_S and \mathbf{W}_S is a $(2N_R + 1) \times (2N_T + 1)$ matrix which has zero-mean independent and identically distributed complex Gaussian random entries with unit variance. Furthermore, using (32), the full correlation matrix of the MIMO channel \mathbf{H} , given by (1), can be written as

$$\mathbf{R} = \left(\mathbf{J}_R^* \mathbf{M}_R \mathbf{J}_R^T \right) \otimes \left(\mathbf{J}_T \mathbf{M}_T \mathbf{J}_T^\dagger \right). \quad (35)$$

For simplicity, here we only consider the modal correlation at the transmitter region and assume the effective communication modes available at the receiver region are uncorrelated, i.e. $\mathbf{M}_{R_x} = \mathbf{I}_{2N_R+1}$. It was shown in [30] that all azimuth power distribution models give very similar correlation values for a given angular spread, especially for small antenna separations. Therefore, without

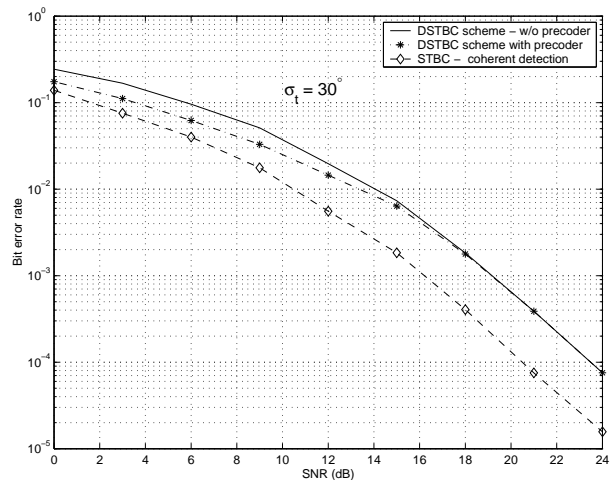


Fig. 11. Precoder performance in non-isotropic scattering environments, $\sigma_t = 30^\circ$ mean AOD $\phi_0 = 0^\circ$ for a uniform-limited azimuth power distribution at the transmitter. 2×2 MIMO system. Transmit antenna separation 0.1λ and receive antenna separation λ : rate-1 differential STBC.

loss of generality, we restrict our investigation only to the uniform-limited azimuth power distribution, which is defined as follows:

Uniform-limited Azimuth Power Distribution: When the energy is departing uniformly to a restricted range of azimuth angles $\pm\Delta$ around a mean angle of departure (AOD) $\phi_0 \in [-\pi, \pi)$, we have the uniform-limited azimuth power distribution [25]

$$\mathcal{P}(\phi) = \frac{1}{2\Delta}, \quad |\phi - \phi_0| \leq \Delta,$$

where Δ represents the non-isotropic parameter of the azimuth power distribution, which is related to the standard deviation of the distribution (angular spread $\sigma_t = \Delta/\sqrt{3}$). For the above APD, the (m, m') -th entry of \mathbf{M}_T is given by

$$\{\mathbf{M}_T\}_{m,m'} = \text{sinc}((m - m')\Delta) e^{i(m-m')\phi_0}.$$

Figures 11 and 12 show the BER performance of rate-1 differential STBC code with two transmit antennas for the spatial arrangement considered in Section VII-B for transmitter angular spreads $\sigma_t = 30^\circ$ and 10° about the mean AOD $\phi_0 = 0^\circ$. The channel is modeled using (1) and (34).

From Figures 11 and 12 it is observed that in the presence of non-isotropic scattering at the transmitter, proposed precoding scheme provides significant BER improvements at low SNRs. To further improve the performance, following Section V, a precoding scheme can be easily derived by including the non-isotropic scattering parameters (angular spreads and mean AOA/AOD) at both ends of the MIMO channel. Unlike in the fixed precoding scheme, modified scheme will require the receiver to estimate and feedback scattering distribution parameters to the transmitter whenever there is a change in these parameters.

VIII. PERFORMANCE IN OTHER CHANNEL MODELS

Simulation results presented in previous sections used the channel model $\mathbf{H} = \mathbf{J}_R \mathbf{H}_S \mathbf{J}_T^\dagger$, which is derived based

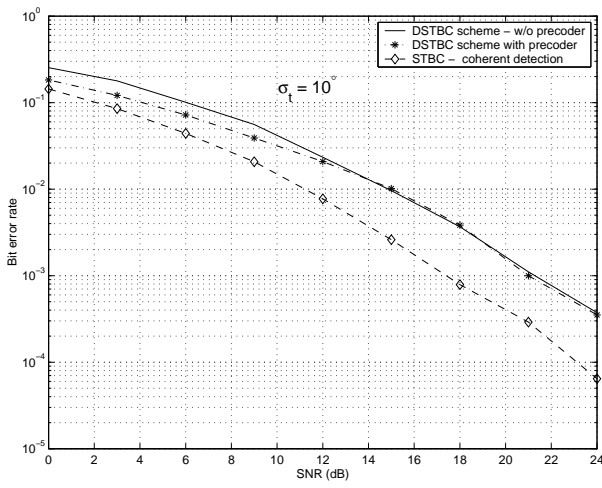


Fig. 12. Precoder performance in non-isotropic scattering environments, $\sigma_t = 10^\circ$ mean AOD $\phi_0 = 0^\circ$ for a uniform-limited azimuth power distribution at the transmitter. 2×2 MIMO system. Transmit antenna separation 0.1λ and receive antenna separation λ : rate-1 differential STBC.

on plane wave propagation theory, to simulate the underlying channels between transmit and receive antennas. In this section we analyze the performance of precoding schemes (coherent and differential) derived in this paper applied on other *statistical channel models* proposed in the literature. In particular we are interested on channel models that are consistent with wave propagation. MISO and MIMO channel models proposed by Chen et al. [31] and Abdi et al. [32], respectively are two such example channel models. Sections VIII-A and VIII-B provide simulation results of coherent STBC applied on Chen's MISO channel model and differential STBC applied on Abdi's MIMO channel model, respectively. In following simulations, precoders are derived using \mathbf{J}_T and \mathbf{J}_R for given antenna configurations and the underlying channel \mathbf{H} is simulated using Chen et al. and Abdi et al. channel models.

A. Chen et al.'s MISO Channel Model

Fig. 13 depicts the MISO channel model proposed by Chen et al., where the space-time cross correlation between two antenna elements at the transmitter is given by

$$[\mathbf{R}(\tau)]_{m,n} = \exp\left[j\frac{2\pi}{\lambda}(d_m - d_n)\right] \times J_0\left[2\pi\sqrt{\left(f_D\tau\cos\gamma + \frac{z_{mn}^c}{\lambda}\right)^2 + \left(f_D\tau\sin\gamma - \frac{z_{mn}^s}{\lambda}\right)^2}\right] \quad (36)$$

with

$$z_{mn}^c = \frac{2a}{d_m + d_n} [d_{mn}^{sp} - (d_m - d_n) \cos\alpha_{mn} \cos\beta_{mn}],$$

$$z_{mn}^s = \frac{2a}{d_m + d_n} (d_m - d_n) \cos\alpha_{mn} \sin\beta_{mn},$$

a is the scatterer ring radius, γ is the moving direction of the receiver with respect to the end-fire of the antenna, f_D is the Doppler spread and d_{mn} is the receiver distance to the center of the transmit antenna pair m, n . All other geometric parameters are defined as in Fig. 13.

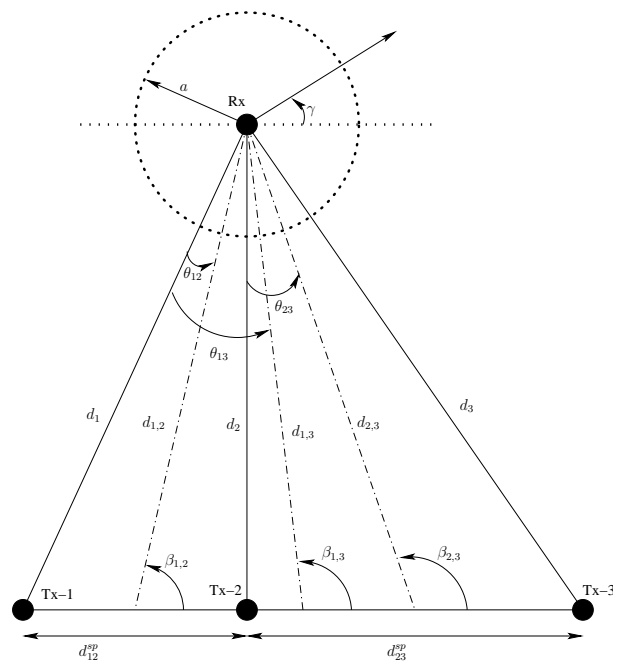


Fig. 13. Scattering channel model proposed by Chen et al. for three transmit and one receive antennas.

Fig. 14 shows the performance of spatial precoder derived in Section IV-A for rate-3/4 coherent STBC with three transmit antennas placed in a ULA configuration. In this simulation, we assume the time-varying channels are undergone Rayleigh fading at the fading rate $f_D T = 0.001$, where T is the codeword period. We set parameters $a = 30\lambda$, $d_{12}^{sp} = d_{23}^{sp} = 0.2\lambda$, $d_{12} = 1000\lambda$, $\gamma = 20^\circ$ and $\beta_{1,2} = 60^\circ$. All other geometric parameters of the model in Fig. 13 can be easily determined from these parameters by using simple trigonometry. In this simulation, a realization of the underlying space-time MIMO channel is generated using (34) and (36). From Fig. 14 we observed that proposed spatial precoding scheme gives significant performance improvements for time-varying channels. For example, at 0.05 BER, performance of the spatially precoded system is 1dB better than that of the non-precoded system.

B. Abdi et al.'s MIMO Channel Model

In this model, space-time cross correlation between two distinct antenna element pairs at the receiver and transmitter is given by

$$[\mathbf{R}(\tau)]_{lp,mq} = \frac{\exp[jc_{pq}\cos(\alpha_{pq})]}{I_0(\kappa)} \times I_0\left(\left\{\kappa^2 - a^2 - b_{lm}^2 - c_{pq}^2\Delta^2\sin^2(\alpha_{pq}) + 2ab_{lm}\cos(\beta_{lm} - \gamma) + 2c_{pq}\Delta\sin(\alpha_{pq}) \times [a\sin(\gamma) - b_{lm}\sin(\beta_{lm})] - j2\kappa[a\cos(\mu - \gamma) - b_{lm}\cos(\mu - \beta_{lm}) - c_{pq}\Delta\sin(\alpha_{pq})\sin(\mu)]\right\}^{1/2}\right), \quad (37)$$

where $a = 2\pi f_D \tau$, $b_{lm} = 2\pi d_{lm}/\lambda$, $c_{pq} = 2\pi \delta_{pq}/\lambda$; f_D is the Doppler shift; μ is the mean angle of arrival at the receiver;

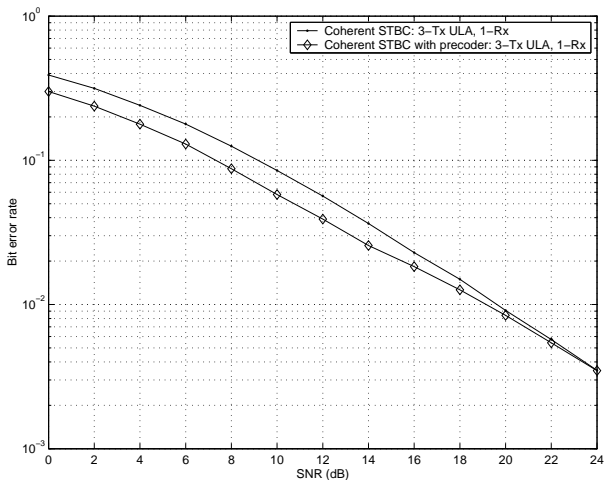


Fig. 14. Spatial precoder performance with three transmit and one receive antennas for 0.2λ minimum separation between two adjacent transmit antennas placed in a uniform linear array, using Chen et al's channel model: rate-3/4 coherent STBC.

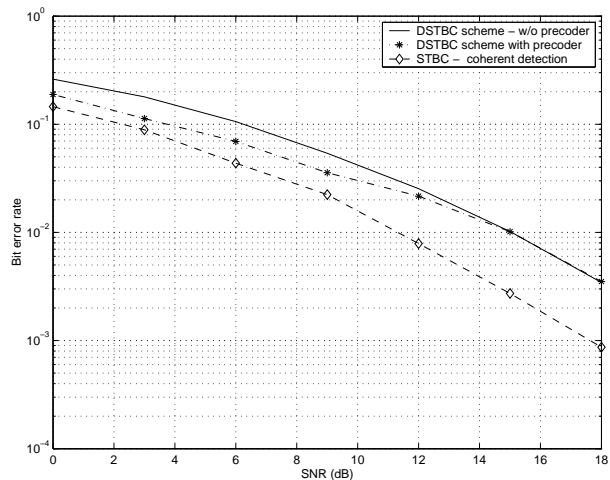


Fig. 16. Spatial precoder performance with two transmit and two receive antennas using Abdi et al's channel model: rate-1 differential STBC.

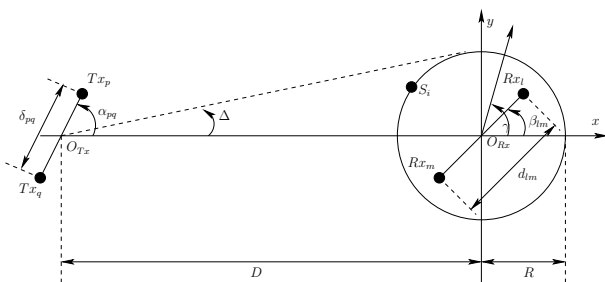


Fig. 15. Scattering channel model proposed by Abdi *et al.* for two transmit and two receive antennas.

κ controls the spread of the AOA; and γ is the direction of motion of the receiver. Other geometric parameters are defined in Fig. 15. Note that this model also captures the non-isotropic scattering at the transmitter via Δ and the model is valid only for small Δ [32].

Fig. 16 shows the performance of spatial precoder derived in Section V-A for rate-1 differential STBC with two transmit and two receive antennas for a stationary receiver (i.e. $f_D = 0$). In this simulation we set $\delta_{12} = 0.1\lambda$, $d_{12} = \lambda$ and $\alpha_{12} = \beta_{12} = 0^\circ$. We assume the scattering environment surrounding the receiver antenna array is rich, i.e., $\kappa = 0$ and the non-isotropic factor Δ at the transmitter is 10° . We assume the scattering channel satisfies the power distribution condition (33). A realization of the underlying MIMO channel is generated using (34) and (37). It is observed that our precoding scheme based on antenna configuration details give promising improvements for low SNR when the underlying channel is modeled using Abdi's channel model. Therefore, using the previous results from Chen's channel model and the current results, we can come to the conclusion that our fixed spatial precoding scheme can be applied to any general wireless communication system.

IX. CONCLUDING REMARKS

In this paper, by exploiting the spatial dimension of a MIMO channel we have proposed spatial precoding schemes for coherent and differential space-time block coded systems. Precoders are derived by minimizing certain upper bounds for the PEP subject to a transmit power constraint and assuming an isotropic scattering environment surrounding the transmit and receive antenna arrays. The proposed precoders are designed based on previously utilized fixed and known parameters of MIMO channels, the antenna spacing and antenna placement details. Therefore, with these schemes the transmitter does not require any feedback of channel state information from the receiver, which is an added advantage over the other precoding schemes found in the literature. Since the precoder is fixed for fixed antenna configurations, proposed precoding schemes can be applied in non-stationary scattering channels as well as stationary scattering channels.

We showed that proposed precoding schemes reduce the detrimental effects of non-ideal antenna placement and improve the performance of space-time coded MIMO systems. Precoders achieve these performance improvements by virtually arranging antennas into an optimal configuration as such the spatial correlation between all antenna elements is minimum. For 1-D arrays (ULA), we observed that precoder gives scope for improvement at high SNRs, but for 2-D arrays (UCA), improvements are only seen at low SNRs.

Although the proposed precoders are derived for isotropic scattering environments, we observed that these precoders give significant performance improvements in non-isotropic scattering environments. Based on the performance improvements we observed, we believe that proposed schemes can be applied on uplink transmission of a mobile communication system as the proposed schemes can effectively reduce the effects due to insufficient antenna spacing and antenna placement at the mobile unit.

PROOF OF PEP UPPER BOUND: COHERENT RECEIVER

The conditional average pairwise error probability $P(\mathbf{S}_i \rightarrow \mathbf{S}_j)$, defined as the probability that the receiver erroneously decides in favor of \mathbf{S}_j when \mathbf{S}_i was actually transmitted for a given channel, is upper bounded by the *Chernoff bound* [3]

$$P(\mathbf{S}_i \rightarrow \mathbf{S}_j | \mathbf{h}) \leq \exp\left(-\frac{\bar{\gamma}}{4} d_h^2(\mathbf{S}_i, \mathbf{S}_j)\right), \quad (38)$$

where $d_h^2(\mathbf{S}_i, \mathbf{S}_j) = \mathbf{h}[\mathbf{I}_{n_R} \otimes \mathbf{S}_\Delta] \mathbf{h}^\dagger$, $\mathbf{S}_\Delta = \mathbf{F}_d(\mathbf{S}_i - \mathbf{S}_j)(\mathbf{S}_i - \mathbf{S}_j)^\dagger \mathbf{F}_d^\dagger$, $\mathbf{h} = (\text{vec}(\mathbf{H}^T))^T$ a row vector and $\bar{\gamma} = E_s/\sigma_n^2$ is the average SNR at each receiver antenna. To compute the average PEP, we average (38) over the joint distribution of \mathbf{h} . Assume \mathbf{h} is a proper complex⁸ $n_T n_R$ -dimensional Gaussian random vector with mean $\mathbf{0}$ and covariance matrix $\mathbf{R}_H = E\{\mathbf{h}^\dagger \mathbf{h}\}$, then the pdf of \mathbf{h} is given by [33]

$$p(\mathbf{h}) = \frac{1}{\pi^{n_T n_R} |\mathbf{R}_H|} \exp\{-\mathbf{h} \mathbf{R}_H^{-1} \mathbf{h}^\dagger\},$$

provided that \mathbf{R}_H is non-singular. Then the average PEP is bounded as follows

$$P(\mathbf{S}_i \rightarrow \mathbf{S}_j) \leq \frac{1}{\pi^{n_T n_R} |\mathbf{R}_H|} \int \exp\{-\mathbf{h} \mathbf{R}_0^{-1} \mathbf{h}^\dagger\} d\mathbf{h} \quad (39)$$

where $\mathbf{R}_0^{-1} = (\frac{\bar{\gamma}}{4} \mathbf{I}_{n_R} \otimes \mathbf{S}_\Delta + \mathbf{R}_H^{-1})$. Assume \mathbf{R}_H is non-singular (positive definite), therefore the inverse \mathbf{R}_H^{-1} is positive definite, since the inverse matrix of a positive definite matrix is also positive definite [22, page 142]. Also note that \mathbf{S}_Δ is Hermitian and it has positive eigenvalues (through code construction, e.g. [3]), therefore \mathbf{S}_Δ is positive definite, hence $\mathbf{I}_{n_R} \otimes \mathbf{S}_\Delta$ is also positive definite. Therefore \mathbf{R}_0^{-1} is positive definite and hence \mathbf{R}_0 is non-singular. Using the normalization property of Gaussian pdf

$$\frac{1}{\pi^{n_T n_R} |\mathbf{R}_0|} \int \exp\{-\mathbf{h} \mathbf{R}_0^{-1} \mathbf{h}^\dagger\} d\mathbf{h} = 1,$$

we can simplify (39) to

$$P(\mathbf{S}_i \rightarrow \mathbf{S}_j) \leq \frac{|\mathbf{R}_0|}{|\mathbf{R}_H|} = \frac{1}{|\mathbf{R}_0^{-1} \mathbf{R}_H|},$$

or equivalently

$$P(\mathbf{S}_i \rightarrow \mathbf{S}_j) \leq \frac{1}{|\mathbf{I}_{n_T n_R} + \frac{\bar{\gamma}}{4} \mathbf{R}_H [\mathbf{I}_{n_R} \otimes \mathbf{S}_\Delta]|}.$$

APPENDIX II

PROOF OF GENERALIZED WATER-FILLING SOLUTION FOR $n_R = 2$ RECEIVER ANTENNAS

Let $n_R = 2$ in (18b), then we obtain the second-order polynomial $r_1 r_2 v_c t_i^2 q_i^2 + (v_c t_i (r_1 + r_2) - 2r_1 r_2 t_i^2) q_i + (v_c - r_1 t_i - r_2 t_i)$ in q which has roots $q_{i,1} = A + \sqrt{K}$ and $q_{i,2} = A - \sqrt{K}$, where A and K are given by (20). Then the

⁸To be proper complex, the mean of both the real and imaginary parts of \mathbf{H}_S must be zero and also the cross-correlation between real and imaginary parts of \mathbf{H}_S must be zero.

product $q_{i,1} q_{i,2} = (v_c - r_1 t_i - r_2 t_i)/r_1 r_2 v_c t_i^2$.

Case 1: $q_{i,1} q_{i,2} > 0 \Rightarrow v_c > t_i(r_1 + r_2)$. In this case, both roots are either positive or negative. Let $v_c = \alpha t_i(r_1 + r_2)$, where $\alpha > 1$. Then $A = -t_i^2 \alpha [(r_1 + r_2)^2 - 2r_1 r_2 / \alpha] < 0$ for all $\alpha > 1$. Since $K > 0$, $q_{i,2} < 0$, thus $q_{i,1}$ must also be negative to hold $v_c > t_i(r_1 + r_2)$. Therefore, when $v_c > t_i(r_1 + r_2)$, the optimum q_i is zero to hold the inequality constraints of (16).

Case 2: $q_{i,1} q_{i,2} < 0 \Rightarrow v_c < t_i(r_1 + r_2)$. In this case, we always have one positive root and one negative root. Assume $q_{i,1} > 0$ and $q_{i,2} < 0$ and let $v_c = \alpha t_i(r_1 + r_2)$, where $0 < \alpha < 1$. For $q_{i,1}$ to positive, we need to prove that $\sqrt{K} > t_i^2 \alpha [(r_1 + r_2)^2 - 2r_1 r_2 / \alpha]$ for $0 < \alpha < 1$. Instead, we show that

$$\sqrt{K} < t_i^2 \alpha [(r_1 + r_2)^2 - 2r_1 r_2 / \alpha], \quad (40)$$

only when $\alpha > 1$. Note that, since $K > 0$, (40) can be squared without affecting to the inequality sign. Therefore squaring (40) and further simplification to it yields $\alpha > 1$. This proves that $q_{i,1} > 0$ and $q_{i,2} < 0$ when $v_c < t_i(r_1 + r_2)$ and the optimum solution to (16) is given by $q_{i,1}$.

APPENDIX III

PROOF OF GENERALIZED WATER-FILLING SOLUTION FOR $n_R = 3$ RECEIVER ANTENNAS

Let $n_R = 3$ in (18b), then we obtain the third-order polynomial $a_3 q_i^3 + a_2 q_i^2 + a_1 q_i + a_0$ in q_i which has roots [34]

$$\begin{aligned} q_{i,1} &= -\frac{a_2}{3} + (S + T), \\ q_{i,2} &= -\frac{a_2}{3} - \frac{1}{2}(S + T) + \frac{i\sqrt{3}}{2}(S - T), \\ q_{i,3} &= -\frac{a_2}{3} - \frac{1}{2}(S + T) - \frac{i\sqrt{3}}{2}(S - T), \end{aligned}$$

where $S \pm T = \left[R + \sqrt{Q^3 + R^2} \right]^{\frac{1}{3}} \pm \left[R - \sqrt{Q^3 + R^2} \right]^{\frac{1}{3}}$ and all other variables are as defined in Section IV-D, then the product $q_{i,1} q_{i,2} q_{i,3} = (r_1 t_i + r_2 t_i + r_3 t_i - v_c)/r_1 r_2 r_3 v_c t_i^3$.

Case 1: $q_{i,1} q_{i,2} q_{i,3} < 0 \Rightarrow v_c > t_i(r_1 + r_2 + r_3)$. Let $v_c = \alpha t_i(r_1 + r_2 + r_3)$, where $\alpha > 1$. For $\alpha > 1$, it can be shown that $(Q^3 + R^2) > 0$, hence $q_{i,1} < 0$ and $q_{i,2}, q_{i,3} \in \mathbb{C}$. Therefore, when $v_c > t_i(r_1 + r_2 + r_3)$, the optimum q_i is zero.

Case 2: $q_{i,1} q_{i,2} q_{i,3} > 0 \Rightarrow v_c < t_i(r_1 + r_2 + r_3)$. Let $v_c = \alpha t_i(r_1 + r_2 + r_3)$, where $0 < \alpha < 1$. For $0 < \alpha < 1$, it can be shown that $(Q^3 + R^2) < 0$ and $R^{\frac{1}{3}} > \frac{a_2}{6}$, hence we get two negative roots $q_{i,2}, q_{i,3} < 0$ and one positive root $q_{i,1} > 0$ as the roots of cubic polynomial. Therefore, when $v_c < t_i(r_1 + r_2 + r_3)$, the optimum solution to (16) is given by $q_{i,1}$.

PROOF OF THE CONDITIONAL MEAN AND THE CONDITIONAL VARIANCE OF $u = 2\text{Re}\{\mathbf{w}(k)\Delta_{i,j}^\dagger \mathbf{y}^\dagger(k-1)\}$

A. Proof of Conditional Mean

Mean of u condition on the received signal $\mathbf{y}(k-1)$ can be written as

$$\begin{aligned}\bar{m}_{u|\mathbf{y}(k-1)} &= E \left\{ 2\text{Re} \left\{ \mathbf{w}(k)\Delta_{i,j}^\dagger \mathbf{y}^\dagger(k-1) \right\} \mid \mathbf{y}(k-1) \right\}, \\ &= 2\text{Re} \left\{ E \left\{ \mathbf{w}(k) \mid \mathbf{y}(k-1) \right\} \Delta_{i,j}^\dagger \mathbf{y}^\dagger(k-1) \right\}.\end{aligned}\quad (41)$$

Substituting $\mathbf{w}(k) = \mathbf{n}(k) - \mathbf{n}(k-1)\mathbf{S}_i$ and noting $E\{\mathbf{n}(k) \mid \mathbf{y}(k-1)\} = 0$, (41) can be simplified to

$$\begin{aligned}\bar{m}_{u|\mathbf{y}(k-1)} &= -2\text{Re} \left\{ \bar{m}_{\mathbf{n}(k-1)|\mathbf{y}(k-1)} \mathbf{S}_i \Delta_{i,j}^\dagger \mathbf{y}^\dagger(k-1) \right\}, \\ &= 2\text{Re} \left\{ \bar{m}_{\mathbf{n}(k-1)|\mathbf{y}(k-1)} (\mathbf{I} - \mathbf{S}_i \mathbf{S}_j^\dagger) \mathbf{y}^\dagger(k-1) \right\},\end{aligned}\quad (42)$$

where $\bar{m}_{\mathbf{n}(k-1)|\mathbf{y}(k-1)} = E\{\mathbf{n}(k-1) \mid \mathbf{y}(k-1)\}$. Using the minimum mean square error estimator results given in [35, Section 2.3], we obtain

$$\begin{aligned}\bar{m}_{\mathbf{n}(k-1)|\mathbf{y}(k-1)} &= E\{\mathbf{n}(k-1)\} + [\mathbf{y}(k-1) - E\{\mathbf{y}(k-1)\}] \\ &\quad \times \Sigma_{\mathbf{y}(k-1),\mathbf{y}(k-1)}^{-1} \Sigma_{\mathbf{y}(k-1),\mathbf{n}(k-1)},\end{aligned}$$

where

$$\begin{aligned}\Sigma_{\mathbf{y}(k-1),\mathbf{y}(k-1)} &= E\{\mathbf{y}^\dagger(k-1)\mathbf{y}(k-1)\}, \\ &= E_s \mathcal{X}(k-1)^\dagger \mathbf{R}_H \mathcal{X}(k-1) + \sigma_n^2 \mathbf{I}_{n_T n_R},\end{aligned}\quad (43)$$

and

$$\begin{aligned}\Sigma_{\mathbf{y}(k-1),\mathbf{n}(k-1)} &= E\{\mathbf{y}^\dagger(k-1)\mathbf{n}(k-1)\}, \\ &= \sigma_n^2 \mathbf{I}_{n_T n_R}.\end{aligned}\quad (44)$$

Since $E\{\mathbf{n}(k-1)\} = 0$ and $E\{\mathbf{y}(k-1)\} = 0$, we have

$$\begin{aligned}\bar{m}_{\mathbf{n}(k-1)|\mathbf{y}(k-1)} &= \sigma_n^2 \mathbf{y}(k-1) \\ &\quad \times \left(E_s \mathcal{X}(k-1)^\dagger \mathbf{R}_H \mathcal{X}(k-1) + \sigma_n^2 \mathbf{I} \right)^{-1}.\end{aligned}\quad (45)$$

Substituting (45) for $\bar{m}_{\mathbf{n}(k-1)|\mathbf{y}(k-1)}$ in (42) gives the conditional mean $\bar{m}_{u|\mathbf{y}(k-1)}$.

B. Proof of Conditional Variance

Variance of u condition on the received signal $\mathbf{y}(k-1)$ can be written as

$$\begin{aligned}\sigma_{u|\mathbf{y}(k-1)}^2 &= E\{\|u - \bar{m}_{u|\mathbf{y}(k-1)}\|^2 \mid \mathbf{y}(k-1)\} \\ &= E\left\{ (u - \bar{m}_{u|\mathbf{y}(k-1)})^\dagger (u - \bar{m}_{u|\mathbf{y}(k-1)}) \mid \mathbf{y}(k-1) \right\}.\end{aligned}\quad (46)$$

After some straight forward manipulations we can show

$$\begin{aligned}u - \bar{m}_{u|\mathbf{y}(k-1)} &= 2\text{Re} \left\{ (\mathbf{n}(k) - [\mathbf{n}(k-1) - \bar{m}_{\mathbf{n}(k-1)|\mathbf{y}(k-1)}]) \right. \\ &\quad \left. \times \mathbf{S}_i \Delta_{i,j}^\dagger \mathbf{y}^\dagger(k-1) \right\}.\end{aligned}\quad (47)$$

Substituting (47) for $u - \bar{m}_{u|\mathbf{y}(k-1)}$ in (46) gives (48), shown at the top of the next page, where $\Sigma_{\mathbf{n}(k),\mathbf{n}(k)} = E\{\mathbf{n}^\dagger(k)\mathbf{n}(k)\} = \sigma_n^2 \mathbf{I}$ and

$$\begin{aligned}\Sigma_{\mathbf{n}(k-1)|\mathbf{y}(k-1)} &= \\ &E\{\|\mathbf{n}(k-1) - \bar{m}_{\mathbf{n}(k-1)|\mathbf{y}(k-1)}\|^2 \mid \mathbf{y}(k-1)\}\end{aligned}$$

is the covariance of the noise vector $\mathbf{n}(k-1)$ condition on $\mathbf{y}(k-1)$. Using the minimum mean square error estimator results given in [35], we can write

$$\begin{aligned}\Sigma_{\mathbf{n}(k-1)|\mathbf{y}(k-1)} &= \Sigma_{\mathbf{n}(k-1),\mathbf{n}(k-1)} \\ &\quad - \Sigma_{\mathbf{y}(k-1),\mathbf{n}(k-1)} \Sigma_{\mathbf{y}(k-1),\mathbf{y}(k-1)}^{-1} \Sigma_{\mathbf{y}(k-1),\mathbf{n}(k-1)}, \\ &= \sigma_n^2 \left[\mathbf{I} - \sigma_n^2 \Sigma_{\mathbf{y}(k-1),\mathbf{y}(k-1)}^{-1} \right]\end{aligned}\quad (49)$$

Substituting (43) for $\Sigma_{\mathbf{y}(k-1),\mathbf{y}(k-1)}$ in (49) and then the result in (48b) gives the conditional variance $\sigma_{u|\mathbf{y}(k-1)}^2$.

APPENDIX V

PROOF OF PEP UPPER BOUND: NON-COHERENT RECEIVER

At asymptotically high SNRs, the PEP condition on the received signal $\mathbf{y}(k-1)$ is given by

$$P(\mathbf{S}_i \rightarrow \mathbf{S}_j \mid \mathbf{y}(k-1)) = Q \left(\sqrt{\frac{d_{i,j}^2}{4\sigma_n^2}} \right).$$

Now using the Chernoff bound

$$Q(x) \leq \frac{1}{2} \exp \left(\frac{-x^2}{2} \right),$$

the conditional PEP can be upper bounded by

$$P(\mathbf{S}_i \rightarrow \mathbf{S}_j \mid \mathbf{y}(k-1)) \leq \frac{1}{2} \exp \left(\frac{-d_{i,j}^2}{8\sigma_n^2} \right). \quad (50)$$

To compute the average PEP, we average (50) over the joint distribution of $\mathbf{y}(k-1)$. Assume $\mathbf{y}(k-1)$ is a proper complex Gaussian random vector that has mean $E\{\mathbf{y}(k-1)\} = \mathbf{0}$ and covariance

$$\begin{aligned}\mathbf{R}_{\mathbf{y}(k-1)} &\triangleq E\{\mathbf{y}^\dagger(k-1)\mathbf{y}(k-1)\}, \\ &= E_s \mathcal{X}(k-1)^\dagger \mathbf{R}_H \mathcal{X}(k-1) + \sigma_n^2 \mathbf{I}_{n_T n_R}\end{aligned}\quad (51)$$

If $\mathbf{R}_{\mathbf{y}(k-1)}$ is non-singular, then the pdf of $\mathbf{y}(k-1)$ is given by

$$p(\mathbf{y}(k-1)) = \Omega_y \exp \left\{ -\mathbf{y}(k-1) \mathbf{R}_{\mathbf{y}(k-1)}^{-1} \mathbf{y}^\dagger(k-1) \right\},$$

where $\Omega_y = \pi^{-n_T n_R} / |\mathbf{R}_{\mathbf{y}(k-1)}|$. Averaging (50) over the pdf of $\mathbf{y}(k-1)$, we obtain

$$\begin{aligned}P(\mathbf{S}_i \rightarrow \mathbf{S}_j) &\leq \\ &\frac{\Omega_y}{2} \int \exp \left\{ -\mathbf{y}(k-1) \mathbf{R}_d^{-1} \mathbf{y}^\dagger(k-1) \right\} d\mathbf{y}(k-1),\end{aligned}\quad (52)$$

where

$$\mathbf{R}_d^{-1} = \mathbf{R}_{\mathbf{y}(k-1)}^{-1} + \frac{1}{8\sigma_n^2} \mathbf{D}_{i,j}.$$

Assume \mathbf{R}_H is non-singular (positive definite). It can be shown that both $\mathbf{R}_{\mathbf{y}(k-1)}$ and $\mathbf{D}_{i,j}$ are positive definite. Therefore, \mathbf{R}_d is non-singular. Using the normalization property of Gaussian pdf

$$\frac{1}{\pi^{n_T n_R} |\mathbf{R}_d|} \int \exp \left\{ -\mathbf{y}(k-1) \mathbf{R}_d^{-1} \mathbf{y}^\dagger(k-1) \right\} d\mathbf{y}(k-1) = 1,$$

$$\begin{aligned} \sigma_{u|y(k-1)}^2 &= \mathbb{E} \left\{ \left[2\text{Re} \left\{ \left(\mathbf{n}(k) - [\mathbf{n}(k-1) - \bar{m}_{\mathbf{n}(k-1)}|y(k-1)] \mathcal{S}_i \right) \Delta_{i,j}^\dagger \mathbf{y}^\dagger(k-1) \right\} \right]^\dagger \right. \\ &\quad \times \left. \left[2\text{Re} \left\{ \left(\mathbf{n}(k) - [\mathbf{n}(k-1) - \bar{m}_{\mathbf{n}(k-1)}|y(k-1)] \mathcal{S}_i \right) \Delta_{i,j}^\dagger \mathbf{y}^\dagger(k-1) \right\} \right] \mid \mathbf{y}(k-1) \right\}, \end{aligned} \quad (48a)$$

$$= 2\mathbf{y}(k-1) \Delta_{i,j} \left[\Sigma_{\mathbf{n}(k), \mathbf{n}(k)} - \mathcal{S}_i^\dagger \Sigma_{\mathbf{n}(k-1)} \mathcal{S}_i \right] \Delta_{i,j}^\dagger \mathbf{y}^\dagger(k-1), \quad (48b)$$

we can simplify (52) to

$$P(\mathcal{S}_i \rightarrow \mathcal{S}_j) \leq \frac{|\mathbf{R}_d|}{2|\mathbf{R}_{\mathbf{y}(k-1)}|} = \frac{1}{2|\mathbf{R}_d^{-1} \mathbf{R}_{\mathbf{y}(k-1)}|},$$

or equivalently

$$P(\mathcal{S}_i \rightarrow \mathcal{S}_j) \leq \frac{1}{2 \left| \mathbf{I} + \frac{1}{8} \left(\bar{\gamma} \mathcal{X}(k-1)^\dagger \mathbf{R}_H \mathcal{X}(k-1) + \mathbf{I}_{n_T n_R} \right) \mathbf{D}_{i,j} \right|}.$$

REFERENCES

- [1] I.E. Telatar, "Capacity of multi-antenna gaussian channels," *Tech. Repo., AT&T Bell Labs*, 1995.
- [2] G.J. Foschini and M.J. Gans, "On limits of wireless communications in a fading environment when using multiple antennas," *Wireless Personal Communications*, vol. 6, pp. 311–335, 1998.
- [3] V. Tarokh, N. Seshadri, and A.R. Calderbank, "Space-time codes for high data rate wireless communication: performance criterion and code construction," *IEEE Trans. Info. Theory*, vol. 44, no. 1, pp. 744–765, Mar. 1998.
- [4] S. Alamouti, "A simple transmit diversity technique for wireless communications," *IEEE Trans. Commun.*, vol. 16, no. 8, pp. 1451–1458, Oct. 1998.
- [5] V. Tarokh, H. Jafarkhani, and A.R. Calderbank, "Space-time codes from orthogonal designs," *IEEE Trans. Info. Theory*, vol. 45, no. 5, pp. 1456–1467, July 1999.
- [6] V. Tarokh and H. Jafarkhani, "A differential detection scheme for transmit diversity," *IEEE Journal on Selected Areas in Communications*, vol. 18, no. 7, pp. 1169–1174, July 2000.
- [7] B. L. Hughes, "Differential space-time modulation," *IEEE Trans. Info. Theory*, vol. 46, pp. 2567–2578, Nov. 2000.
- [8] B. M. Hochwald and W. Sweldens, "Differential unitary space-time modulation," *IEEE Trans. Commun.*, vol. 48, no. 12, pp. 2041–2052, Dec. 2000.
- [9] H. Bölcskei and A.J. Paulraj, "Performance of space-time codes in the presence of spatial fading correlation," in *Asilomar Conf. on Signals, Systems, and Computers*, Pacific Grove (CA), Oct. 2000, vol. 1, pp. 687–693.
- [10] M. Uysal and C.N. Georghiades, "Effect of spatial fading correlation on performance of space-time codes," *Electronics Letters*, vol. 37, no. 3, pp. 181–183, Feb. 2001.
- [11] T.A. Latham, M.K. Simon, R.A. Kennedy, and T.D. Abhayapala, "Performance analysis of space-time codes in realistic propagation environments: A moment generating function-based approach," *International Journal on Communications and Networks*, vol. 7, no. 4, pp. 1–12, Dec. 2005.
- [12] H. Sampath and A. Paulraj, "Linear precoding for space-time coded systems with known fading correlations," in *In Proc. Thirty-Fifth Asilomar Conference Signals, Systems and Computers*, Pacific Grove, CA, USA, Nov. 2001, vol. 1, pp. 246–251.
- [13] G.B. Giannakis and S. Zhou, "Optimal transmit-diversity precoders for random fading channels," in *Proc. of GLOBECOM*, San Francisco, CA, Nov. 27 - Dec. 1 2000, vol. 3, pp. 1839–1843.
- [14] Y. Zhao, R. Adve, and T. J. Lim, "Precoding of orthogonal STBC with channel covariance feedback for minimum error probability," in *15th IEEE International Symposium on Personal, Indoor and Mobile Radio Communications PIMRC'2004*, Barcelona, Spain, Sept. 2004.
- [15] A. Hjørungnes, J. Akhtae, and D. Gesbert, "Precoding for space-time block codes in (non-)kronecker correlated MIMO channels," in *12th European Signal Processing Conference, EUSIPCO'2004*, Vienna, Austria, Sept. 2004, pp. 6–10.
- [16] Cai X. and Giannakis G. B., "Differential space-time modulation with transmit-beamforming for correlated MIMO fading channels," in *IEEE International Conference on Acoustics, Speech, and Signal Processing, 2003 (ICASSP '03)*, Apr. 2003, vol. 4, pp. IV–25–28.
- [17] V. K. Nguyen, "Differential encoding technique for multi-antenna systems with correlated rayleigh fading channels," in *IEEE International Conf. on Industrial Tech. (to appear)*, Hong Kong, Dec. 2005.
- [18] T.D. Abhayapala, T.S. Pollock, and R.A. Kennedy, "Spatial decomposition of MIMO wireless channels," in *The Seventh International Symposium on Signal Processing and its Applications*, Paris, France, July 2003, vol. 1, pp. 309–312.
- [19] T.D. Abhayapala, T.S. Pollock, and R.A. Kennedy, "Characterization of 3D spatial wireless channels," in *IEEE Vehicular Technology Conference (Fall), VTC2003*, Orlando, Florida, USA, Oct. 2003, vol. 1, pp. 123–127.
- [20] L. Hanlen and M. Fu, "Wireless communications systems with spatial diversity: a volumetric approach," in *IEEE International Conference on Communications, ICC-2003*, 2003, vol. 4, pp. 2673–2677.
- [21] H.M. Jones, R.A. Kennedy, and T.D. Abhayapala, "On dimensionality of multipath fields: Spatial extent and richness," in *Proc. IEEE Int. Conf. Acoust., Speech, Signal Processing, ICASSP'2002*, Orlando, Florida, May 2002, vol. 3, pp. 2837–2840.
- [22] G.H. Golub and C.F. Van Loan, *Matrix Computations*, The Johns Hopkins University Press, Baltimore and London, third edition, 1996.
- [23] S. Boyd and L. Vandenberghe, *Convex Optimization*, Cambridge University Press, 2004.
- [24] T.A. Latham, T.D. Abhayapala, and R.A. Kennedy, "Fading resistance of orthogonal space-time block codes under spatial correlation," in *IEEE Workshop on Signal Processing Advances in Wireless Communications, SPAWC*, Lisbon, Portugal, July 2004.
- [25] J. Salz and J.H. Winters, "Effect of fading correlation on adaptive arrays in digital mobile radio," *IEEE Trans. Vehic. Technol.*, vol. 42, no. 4, pp. 1049–1057, Nov. 1994.
- [26] M. Kalkan and R.H. Clarke, "Prediction of the space frequency correlation function for base station diversity reception," *IEEE Trans. Vehic. Technol.*, vol. VT-46, no. 1, pp. 176–184, Feb. 1997.
- [27] K.I. Pedersen, P.E. Mogensen, and B.H. Fleury, "Power azimuth spectrum in outdoor environment," *IEEE Electronics Letters*, vol. 33, no. 18, pp. 1583–1584, Aug. 1997.
- [28] T.S. Pollock, "Correlation Modelling in MIMO Systems: When can we Kronecker?," in *Proc. 5th Australian Communications Theory Workshop*, Newcastle, Australia, Feb. 2004, pp. 149–153.
- [29] J.P. Kermaol, L. Schumacher, K.I. Pedersen, P.E. Mogensen, and F. Frederiksen, "A stochastic MIMO radio channel model with experimental validation," *IEEE Journal on Selected Areas in Communications*, vol. 20, no. 6, pp. 1211–1226, Aug. 2002.
- [30] T.S. Pollock, T.D. Abhayapala, and R.A. Kennedy, "Introducing space into MIMO capacity calculations," *Journal on Telecommunications Systems (Kluwer Academic Publishers)*, vol. 24, no. 2, pp. 415–436, 2003.
- [31] T.A. Chen, M.P. Fitz, W.Y. Kuo, M.D. Zoltowski, and J.H. Grimm, "A spacetime model for frequency nonselective rayleigh fading channels with applications to space-time modems," *IEEE Journal on Selected Areas in Communications*, vol. 18, pp. 1175–1190, July 2000.
- [32] A. Abdi and M. Kaveh, "A space-time correlation model for multielement antenna systems in mobile fading channels," *IEEE Journal on Selected Areas in Communications*, vol. 20, pp. 550–560, May 2002.
- [33] N.R. Goodman, "Statistical analysis based on a certain multivariate complex gaussian distribution (an introduction)," *Ann. Math. Statist.*, vol. 34, pp. 152–177, 1963.
- [34] G.A. Korn and T.M. Korn, *Mathematical Handbook for Scientists and Engineers*, Dover, New York, NY, 1968.
- [35] Anderson B.D.O. and Moore J.B., *Optimal Filtering*, Dover Publications, New York, 2005.